

Chapter 3

Optical Receivers and Ideal Performance

Coherent detection of optical signal is first proposed because of its superior receiver sensitivity compared with on-off keying modulation. Equivalent speaking, the mixing of received signal with the local oscillator (LO) laser functions as an optical amplifier without noise enhancement. With the advance of Erbium-doped optical amplifiers (EDFA), coherent detection can still provide better receiver sensitivity than amplified on-off keying. In this chapter, various structures of optical receivers for coherent optical communications are studied. This chapter focuses on performance analysis to validate the receiver sensitivity improvement of coherent optical communications. However, for binary signals limited by amplifier noises, the improvement is limited to about 3 dB.

In a coherent receiver, phase-locked loop (PLL) is required to track the phase of the received signal. In coherent optical communication, receiver with phase tracking is called synchronous receiver. Equivalent to the matched filter receiver in digital communications (Proakis, 2000), receivers with phase tracking always provide the optimal performance.

Without phase tracking, the received signal has a random phase and can be detected based on the power or the envelope of the signal (Proakis, 2000). This type of non-coherent receiver is called asynchronous receiver in coherent optical communication. While the performance is inferior compared with synchronous receiver, asynchronous receiver has simple structure and provides low-cost implementation.

Coherent optical signal can also directly be detected without mixing with LO signal. While on-off keying or, equivalently, amplitude-shift keying (ASK) is detected by a photodiode, both phase- or frequency-modulated signals has directed-detection receiver based on interferometer or optical filter, respectively. Direct-detection receiver may be the simplest receiver with low-cost implementation.

Another types of non-coherent receiver use phase-diversity techniques that combines two signals with a phase difference of 90° . Phase-diversity receiver is non-coherent receiver without the requirement of phase tracking. Equivalently speaking, phase-diversity receiver implements the envelope and power detection by combining optical and electrical techniques.

Other than polarization diversity receivers, to enable the mixing of two optical signals, their polarizations have to be aligned. In general, polarization alignment is provided by electronic control. With optimal combining of the signal from both polarizations, polarization-diversity receivers have the same performance as receiver with polarization tracking.

3.1 Basics Coherent Receiver Structures

The basic structures of PSK and DPSK receivers have been shown in Figs. 1.3 and Fig. 1.4. This section studies each basic type of coherent optical receivers that mix the received signal with the LO laser. The signal-to-noise ratio (SNR) of each receiver types is derived, especially for systems limited by amplifier noises. The SNR is equal to the ratio of optical signal to the amplifier noise per polarization over an optical bandwidth equal to the data rate. For system without optical amplifiers, the SNR is equal to the

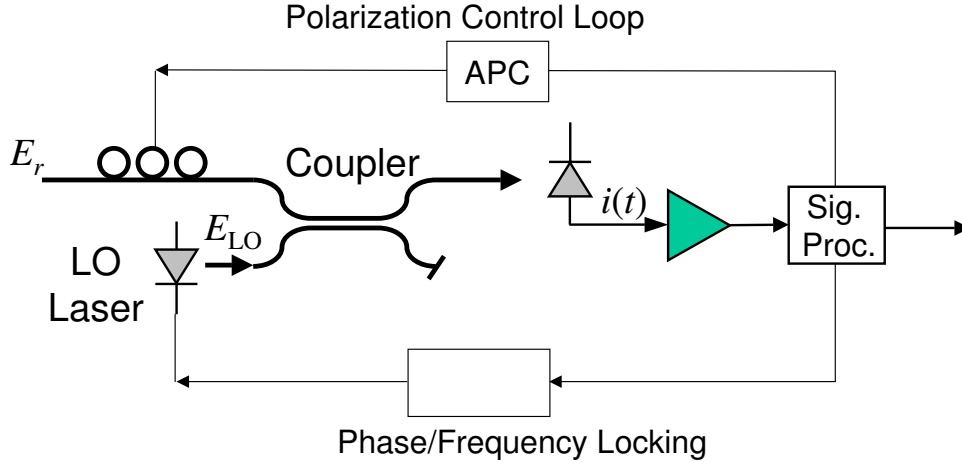


Figure 3.1: A single-branch coherent optical receiver.

number of photons per bit for heterodyne receiver.

3.1.1 Single-Branch Receiver

Figure 3.1 shows a typical structure of a single-branch coherent optical receiver. For optimal optical signal mixing, the polarization of the received signal must be the same as that from LO laser. In Fig. 3.1, automatic polarization control (APC) is used to align the polarization of the received signal to that of LO laser such that they can be mixed with each other. In general, the LO laser is either phase or frequency locking to the received signal. Phase locking is used for homodyne receiver and frequency locking is required for heterodyne receiver for a fixed intermediate frequency (IF). Phase locking is facilitated by an optical phase-locked loop (PLL) and frequency locking is conducted by an automatic frequency control (AFC) loop. The single-branch receiver is the simplest receiver structure. Most early heterodyne receivers used single-branch receiver for its simplicity (Goodwin, 1967, Nussmeier et al., 1974, Oliver, 1961, Peyton et al., 1972, Saito et al., 1981). Instead of 3-dB coupler, those early works used a power beam splitter or a power combiner, function as an 180° optical hybrid, to mix the received signal with LO laser.

A 3-dB coupler is used in Fig. 3.1 to mix the received signal with the LO laser. The input and output relationship of 3-dB coupler is ¹

$$S = \frac{1}{\sqrt{2}} \begin{bmatrix} 1 & 1 \\ 1 & -1 \end{bmatrix}. \quad (3.1)$$

The received signal is assumed to be

$$E_r(t) = [A_s(t)e^{j\phi_s(t)} + n_x(t)]e^{j\omega_c t} \mathbf{x} + n_y(t)e^{j\omega_c t} \mathbf{y} \quad (3.2)$$

where $A_s(t)$ is the modulated amplitude, ω_c is the carrier frequency, and $\phi_s(t)$ is the modulated phase of the transmitted laser, \mathbf{x} is the polarization of the signal, and \mathbf{y} is the polarization orthogonal to \mathbf{x} , $n_x(t)$ and $n_y(t)$ are the amplifier noise in the polarization of \mathbf{x} and \mathbf{y} , respectively. The complex signal of $A_s(t)e^{j\phi_s(t)}$ is the low-pass representation of the signal. $A_s(t)e^{j\phi_s(t)} = \pm A$ and $A_s(t)e^{j\phi_s(t)} = \{0, A\}$ for

¹The input and output relationship can also be

$$S = \frac{1}{\sqrt{2}} \begin{bmatrix} 1 & j \\ 1 & -j \end{bmatrix}.$$

without change the phase relationship. Different input and output relationship for an 180° hybrid may be used in this book for convenient.

PSK and ASK signal, respectively, where A is a real amplitude. Both $n_x(t)$ and $n_y(t)$ are the low-pass representation of the amplifier noise. Here, in this chapter, we assume that laser is a pure coherent source without phase noise. In next chapter, the impact of laser phase noise to coherent modulated signal is analyzed in details. The received signal may have a random phase of θ_0 of $A_s(t)e^{j\phi_s(t)+j\theta_0}$ due to propagation delay. For system with phase tracking using phase-locked loop, we assume that $\theta_0 = 0$ for simplicity when the phase of LO laser tracking out the phase of θ_0 . For system without phase tracking, the phase of θ_0 is included when necessary.

The optical SNR of the received signal is defined as

$$SNR_{o,s} = \frac{E\{|A_s(t)|^2\}}{E\{|n_x(t)|^2\} + E\{|n_y(t)|^2\}} = \frac{P_r}{2S_{n_s}\Delta f_{o,s}}, \quad (3.3)$$

where P_r is the received power, S_{n_s} is the spectral density of the received spontaneous emission in each polarization, and $\Delta f_{o,s}$ is the optical bandwidth of the received optical filter. In the complex representation of $n_x(t) = n_{x1}(t) + jn_{x2}(t)$, the spectral densities of $n_{x1}(t)$ and $n_{x2}(t)$ are the same and equal to $\frac{1}{2}S_{n_s}$.

The LO signal is

$$E_{LO}(t) = [A_L + n_L(t)]e^{j\omega_{LO}t} \quad (3.4)$$

where A_L is the continuous-wave amplitude of LO laser, $n_L(t)$ is the noise of LO laser in the same polarization as the signal, and ω_{LO} is the angular frequency of LO laser. The polarization of received signal of Eq. (3.2) and LO laser of Eq. (3.4) is assumed to be the same using automatic polarization control. The noise of $n_L(t)$ may originate from the optical amplifier used to boost up the LO power or from the relative intensity noise (RIN) of the LO laser. In the LO electric field of Eq. (3.4), the noise at polarization orthogonal to the signal is ignored here simplicity. In practice, the noise from polarization orthogonal to the signal can be filtered by a polarizer, especially at the receiver having a well-control LO laser.

In the single branch receiver of Fig. 3.1, the electric field at the input of the photodiode is $\frac{1}{\sqrt{2}}[E_r(t) + E_{LO}(t)]$, the current of the photodiode is

$$i(t) = \frac{R}{2} |E_r(t) + E_{LO}(t)|^2 + i_{sh} + i_{th}, \quad (3.5)$$

where R is the responsivity of the photodiode, i_{sh} is the photo-current shot-noise, and i_{th} is the received thermal noise of the receiver. In later part of this chapter, other than specific, we ignored thermal noise for simplicity. As an additive noise, the effect of thermal noise can be added to the system afterward. In coherent optical communication systems, thermal noise is considerable having less impact than both shot noise and amplifier noises.

The photodiode responsivity is equal to

$$R = \eta \frac{e}{\hbar\omega_c} \quad (3.6)$$

where $e = 1.6 \times 10^{-19}$ C is the charge per electron, $\hbar\omega_c$ is the energy per photon for light where $\hbar = h/(2\pi)$ with $h = 6.63 \times 10^{-34}$ J s as the Planck constant, η is the quantum efficiency of photodiode that is the average number of electronics generated per a photon.

The photocurrent of Eq. (3.5) is equal to

$$\begin{aligned} i(t) = & \frac{R}{2} \left\{ |A_L + n_L(t)|^2 + |A(t) + n_x(t)|^2 + |n_y(t)|^2 \right\} \\ & + RA_L A_s(t) \cos[\omega_{IF}t + \phi_s(t)] \\ & + R\Re \left\{ [A_L n_x(t) + A_s(t)e^{j\phi_s(t)} n_L(t)] e^{j\omega_{IF}t} \right\} + i_{sh}. \end{aligned} \quad (3.7)$$

In the photocurrent of Eq. (3.7), the intermediate frequency (IF) is $\omega_{\text{IF}} = \omega_c - \omega_{\text{LO}}$. Homodyne system has $\omega_{\text{IF}} = 0$ but heterodyne system has $\omega_{\text{IF}} \neq 0$. The photocurrent of Eq. (3.7) includes the power of LO laser with noise of $|A_L + n_L(t)|^2$, the power of received signal with noise of $|A(t) + n_x(t)|^2$, the spontaneous-spontaneous beating from orthogonal polarization of $|n_y(t)|^2$, the beating of received signal with LO laser of $RA_L A_s(t) \cos[(\omega_c - \omega_{\text{LO}})t + \phi_s(t)]$, LO and spontaneous beating of $A_L n_x(t)$, signal and LO-spontaneous beating of $A_s(t)n_L(t)$, together with shot noise i_{sh} . In the photocurrent of Eq. (3.7), the small effect of the beating of spontaneous noise with shot noise is ignored. If necessary, thermal noise can add to the photocurrent of Eq. (3.7).

In the photocurrent of Eq. (3.7), the signal component is

$$s(t) = RA_L A_s(t) \cos[(\omega_c - \omega_{\text{LO}})t + \phi_s(t)]. \quad (3.8)$$

For heterodyne system with $\omega_{\text{IF}} = \omega_c - \omega_{\text{LO}} \neq 0$, the signal power is

$$P_s = \frac{R^2}{2} P_{\text{LO}} P_r. \quad (3.9)$$

where $P_{\text{LO}} = A_L^2$ is the LO power, $P_r = E\{|A_s(t)|^2\}$ is the received power. In PSK homodyne system with $\omega_c = \omega_{\text{LO}}$ and $A_s(t) = \pm 1$ and $\phi_s(t) = 0$, we get

$$P_s = R^2 P_{\text{LO}} P_r. \quad (3.10)$$

Comparing the the signal power of Eq. (3.9) for heterodyne system with the signal power of Eq. (3.10) for homodyne system, homodyne system has twice the signal power of heterodyne system. Conventionally, it was generally believe that homodyne system is 3 dB better than heterodyne system (Betti et al., 1995, Cvijetic, 1996, Hooijmans, 1994, Okoshi and Kikuchi, 1988, Ryu, 1995). However, for system dominant by optical amplifier noise, heterodyne system generally has the same performance as a homodyne system.

The dominant noise source for the single-branch receiver depends on the system configuration. In the usual case that the LO power is larger than the received power, i.e., $P_{\text{LO}} \gg P_r$, the dominant noise is usually LO-spontaneous beating noise. The beating of LO laser with the spontaneous emission of either $n_L(t)$ or $n_x(t)$ is given by $R\Re\{A_L n_x(t) e^{j\omega_{\text{IF}} t}\}$ in the photocurrent of Eq. (3.7).

If the spontaneous emissions of LO source and signal are not negligible with $n_L(t) \neq 0$ and $n_x(t) \neq 0$, the LO-spontaneous emission beating including two components of $R\Re\{A_L n_L(t)\}$ from $\frac{R}{2}|A_L + n_L(t)|^2$ and $R\Re\{A_L n_x(t) e^{j\omega_{\text{IF}} t}\}$. If the optical bandwidth of $n_L(t)$ is $\Delta f_{o,L}$ centered around ω_L , the bandwidth of $R\Re\{A_L n_L(t)\}$ is less than $\Delta f_{o,L}/2$. For heterodyne system with $f_{\text{IF}} = \omega_{\text{IF}}/(2\pi) \neq 0$ and $f_{\text{IF}} > \frac{1}{2}\Delta f_{o,L} + B_d$, an electric filter can be designed such that the beating of A_L with $n_L(t)$ does not affect the performance of the system, where B_d is the symbol rate of the data channel. In homodyne system with $\omega_{\text{IF}} = f_{\text{IF}} = 0$, the beating of A_L with $n_L(t)$ always contributes to the noise of the system.

In the LO and $n_x(t)$ beating of $R\Re\{A_L n_x(t) e^{j(\omega_{\text{IF}})t}\}$, if the optical bandwidth of $n_x(t)$ is $\Delta f_{o,s}$ centered around ω_c , the upper and lower frequency of LO and $n_x(t)$ is $f_{\text{IF}} \pm \frac{1}{2}\Delta f_{o,s}$. Figure 3.2 illustrates the effect of the optical filter bandwidth of $\Delta f_{o,s}$ on the beating of LO laser with received spontaneous emission of $n_x(t)$. Without loss of generality and assume that $f_{\text{IF}} > 0$ as in Fig. 3.2, the lower frequency of $f_{\text{IF}} - \frac{1}{2}\Delta f_{o,s}$ may be a negative frequency. The negative frequency noise affects the system if $f_{\text{IF}} - \frac{1}{2}\Delta f_{o,s}$ falls into the data bandwidth of $-f_{\text{IF}} + B_d$. The upper two traces of Fig. 3.2 show the case when the optical bandwidth of $n_x(t)$ is small and comparable to twice the data bandwidth of B_d . The beating noise is bandpass noise centered at f_{IF} . The lower two traces of Fig. 3.2 show the case when the optical bandwidth of $n_x(t)$ is larger than the data bandwidth of B_d . With $f_{\text{IF}} - \frac{1}{2}\Delta f_{o,s} < 0$, the beating noise extends to $f_{\text{IF}} - \frac{1}{2}\Delta f_{o,s}$. In the worse case of having a wide-bandwidth received optical filter, the beating noise centered at f_{IF} with a bandwidth of $2B_d$ is doubled compared with case of narrow-bandwidth filter.

The diagram of Fig. 3.2, the data bandwidth is assumed to be $2B_d$. In practical system, depending on linecode or spectral filtering, the data bandwidth may vary.

The beating noise is not doubled if

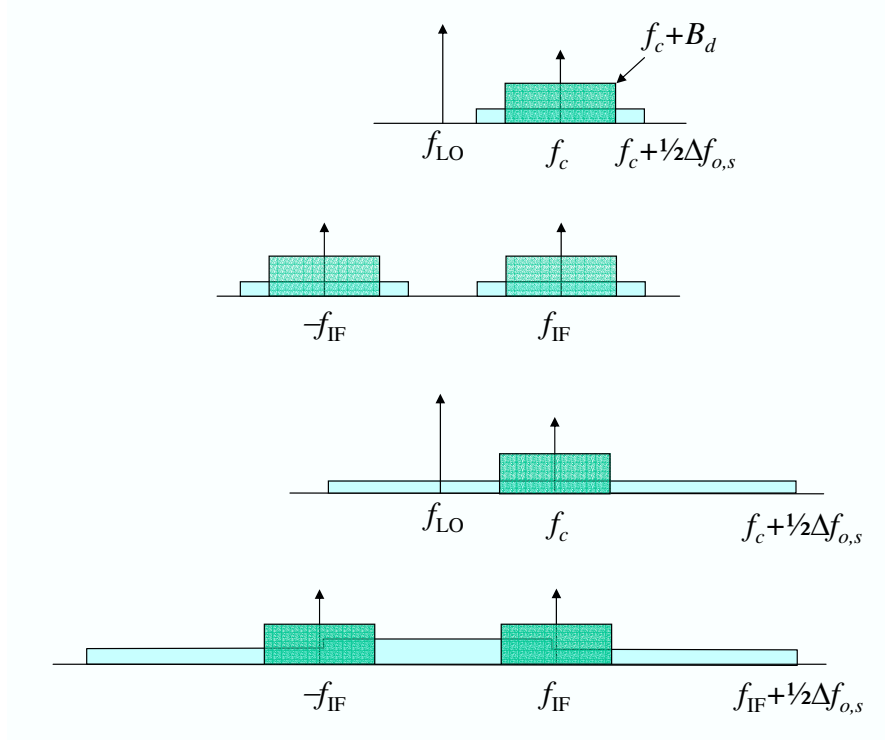


Figure 3.2: An illustration of the effects of receiver filter bandwidth of $\Delta f_{o,s}$ on LO-spontaneous beat noise. The optical bandwidth of $\Delta f_{o,s}$ is comparable (upper two figures) and much larger than (lower two figures) than twice the data bandwidth.

$$\frac{1}{2}\Delta f_{o,s} - f_{IF} < f_{IF} - B_d \quad (3.11)$$

or

$$f_{IF} > \frac{1}{4}(\Delta f_{o,s} + 2B_d). \quad (3.12)$$

In homodyne system, the LO and $n_x(t)$ beating is within the frequency of $\pm \frac{1}{2}\Delta f_{o,s}$ and contributes into the positive and negative noise frequency twice. Because the power of homodyne receiver twice that of heterodyne receiver by comparing Eq. (3.9) and Eq. (3.10), with the condition of Eq. (3.12), the SNR at the output of a single-branch receiver of homodyne and heterodyne systems is the same. However, without the condition of Eq. (3.12), the noise of homodyne and heterodyne system is the same, homodyne system is 3 dB better than heterodyne system.

Under the condition of Eq. (3.12), heterodyne and homodyne system has the same performance. With proper design, a coherent system with optical amplifiers is generally limited by the beating of LO signal of A_L with received spontaneous emission of $n_x(t)$. When the optical filter has a bandwidth of $\Delta f_{o,s} = 2B_d$, the IF must be larger than $f_{IF} > B_d$. In the limit, the narrowest optical bandwidth if $\Delta f_{o,s} = B_d$ for an optical match filter for NRZ signal. However, for RZ signal with small duty cycle, the optical bandwidth of an optical match filter is larger than the data-rate of B_d .

In general, the conditional of Eq. (3.12) is an approximation. While the bandwidth of $f_{IF} \pm B_d$ is a good approximation, ideal since pulse has the bandwidth of $f_{IF} \pm \frac{1}{2}B_d$ but RZ pulse has bandwidth wider than $2B_d$. The condition of Eq. (3.12) is a good approximation for most practical cases.

Assuming the condition of Eq. (3.12), when the LO laser of A_L beats with $n_x(t)$, the beating noise is

$$RA_L n_{x1}(t) \cos(\omega_{IF}t) - RA_L n_{x2}(t) \sin(\omega_{IF}t) \quad (3.13)$$

where $n_s(t) = n_{x1}(t) + jn_{x2}(t)$ with $E\{n_{x1}^2(t)\} = E\{n_{x2}^2(t)\} = \frac{1}{2}S_{n_s}B_d$. The LO laser source of A_L beating with $n_x(t)$ induces an electronic noise with spectrum density of

$$N_{A_L-n_s} = \frac{1}{2}R^2S_{n_s}P_{LO}. \quad (3.14)$$

The LO laser source of A_L beating with $n_L(t)$ induces electronic noise with spectrum density of

$$N_{A_L-n_L} = \frac{1}{2}R^2S_{n_L}P_{LO}, \quad (3.15)$$

where S_{n_L} is the spectrum density of the spontaneous of $n_L(t)$ at optical domain.

The optical signal-to-noise ratio (SNR) of LO laser source can be defined as

$$\text{SNR}_{o,LO} = \frac{P_{LO}}{2S_{n_L}\Delta f_{o,L}}. \quad (3.16)$$

Note that the above SNR assumes that amplifier noises have two polarizations, in contract of LO electric field of Eq. (3.4).

Because the receiver should not induce noise into the system, the system must be designed for $N_{A_L-n_s} > 10 \times N_{A_L-n_L}$, or $S_{n_s} > 10 \times S_{n_L}$, where the factor of 10 is for the condition that the additional penalty due to $n_L(t)$ is less than 0.5 dB. For an optical SNR defined for the same bandwidth of $\Delta f_{o,s} = \Delta f_{o,L}$, we need

$$\frac{\text{SNR}_{o,LO}}{\text{SNR}_{o,s}} > 10 \times \frac{P_{LO}}{P_r}. \quad (3.17)$$

with the condition of $P_{LO} \gg P_r$, the required optical SNR of the LO source must be much larger than that of the received signal.

If the optical SNR of LO source is not substantially larger than that of the signal source, the system is dominated by noise from the LO source. The noise of the LO source may be induced by an optical amplifier that boost up the power of the LO laser or the RIN of LO laser. In order to cancel the LO laser noise, a balanced receiver can be used instead. Because balanced receiver has better performance than single-branch receiver, the analysis of this book usually focuses on balanced receiver.

In the receiver of Fig. 3.1, many methods can provide automatic polarization control (APC) (Aarts and Khoe, 1989, Martinelli and Chipman, 2003, Noe et al., 1988a, 1991, Okoshi, 1985, Walker and Walker, 1990). The polarization control algorithm should be able to provide endless polarization control without reset.

3.1.2 Balanced Receiver

Figure 3.3 show a dual-photodiode balanced receiver that doubles the signal power and eliminates the noise from LO laser source. Similar to single branch receiver of Fig. 3.1, balanced receiver of Fig. 3.3 requires both automatic polarization control (APC) and phase or frequency locking. The electric field at the input of the first photodiode is $\frac{1}{\sqrt{2}}[E_r(t) + E_{LO}(t)]$, the same as Eq. (3.5), the current of the photodiode is

$$i_1(t) = \frac{R}{2}|E_r(t) + E_{LO}(t)|^2 + i_{sh1}. \quad (3.18)$$

where i_{sh1} is the shot noise. The electric field at the input of the second photodiode is $\frac{1}{\sqrt{2}}[E_r(t) - E_{LO}(t)]$, the current of the photodiode is

$$i_2(t) = \frac{R}{2}|E_r(t) - E_{LO}(t)|^2 + i_{sh2}. \quad (3.19)$$

where i_{sh2} is the shot noise.

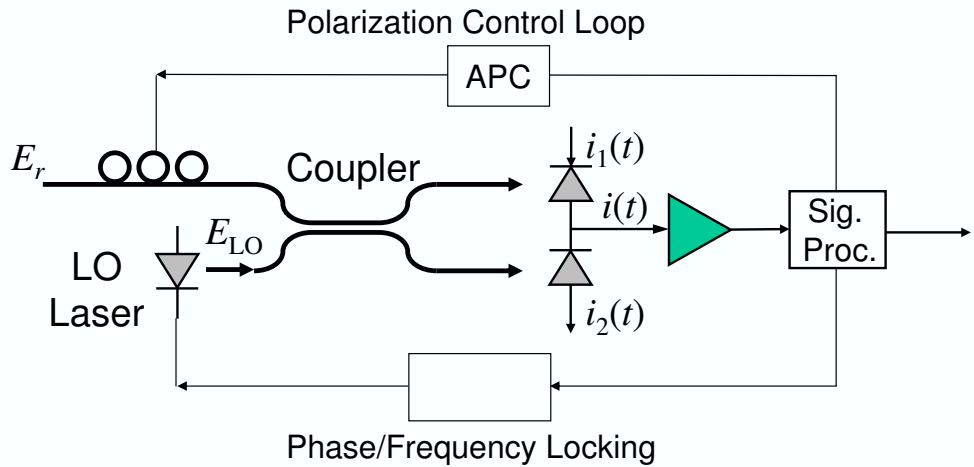


Figure 3.3: A dual-photodiode balanced receiver for coherent optical communication.

In both photocurrents of Eq. (3.18) and Eq. (3.19), we assume that the two photodiodes are identical with same responsivity and the 3-dB coupler or 180° optical hybrid is exactly 3-dB without loss. The overall photocurrent is

$$i(t) = i_1(t) - i_2(t) = 2R\Re\{E_r(t) \cdot E_{LO}^*(t)\} + i_{sh} \quad (3.20)$$

or

$$i(t) = 2RA_L A_s(t) \cos[\omega_{IF}t + \phi_s(t)] + 2R\Re\left\{\left[A_L n_x(t) + A_s(t)e^{j\phi_s(t)}n_L(t)\right]e^{j\omega_{IF}t}\right\} + i_{sh}. \quad (3.21)$$

where $i_{sh} = i_{sh1} - i_{sh2}$ is the overall shot noise.

In the photocurrent of Eq. (3.21), the noise from the LO laser of $n_L(t)$ contributes to the system noise because of the beating term of $2R\Re\{A_s(t)n_L(t)e^{j\omega_{IF}t+j\phi_s(t)}\}$ with a spectral density of

$$N_{A_s-n_L} = 2R^2 S_{n_L} P_r. \quad (3.22)$$

Comparing with the LO-spontaneous beating noise of

$$N_{A_L-n_s} = 2R^2 S_{n_s} P_{LO}, \quad (3.23)$$

as long as the optical SNR has the relationship of $\text{SNR}_{o,LO} > 10 \times \text{SNR}_{o,s}$, we have $N_{A_L-n_s} > 10 \times N_{A_s-n_L}$ such that the signal and LO noise beating does not provide a penalty more than 0.5 dB. Even when a boost amplifier is used, the LO laser required low-gain optical amplifier but the signal usually passes through chain of many optical amplifiers. The optical SNR of the LO signal is usually much larger than that of the received signal. The signal and spontaneous emission beating of $N_{A_s-n_L}$ is usually much smaller than $N_{A_L-n_s}$.

The signal component of the photocurrent of Eq. (3.21) is

$$s(t) = 2RA_L A_s(t) \cos[\omega_{IF}t + \phi_s(t)]. \quad (3.24)$$

Similar to the illustration of Fig. 3.2, the same as single-branch receiver, a heterodyne balanced receiver also required a received optical filter with the condition of Eq. (3.12) without doubling the LO-spontaneous beating noise. For system limited by optical amplifier noise, the performance of heterodyne and homodyne receiver is the same if the conditional of Eq. (3.12) is satisfied.

Here, we analyze the SNR of a heterodyne system with amplifier noise with the condition of Eq. (3.12) for a balanced receiver, the signal power is

$$P_s = 2R^2 P_{LO} P_r. \quad (3.25)$$

The noise variance at a balanced receiver includes LO-spontaneous beating noise of

$$\sigma_{LO-sp}^2 = 2R^2 P_{LO} S_{n_s} B_d, \quad (3.26)$$

and the signal-LO spontaneous beating noise variance of

$$\sigma_{sig.-LOsp}^2 = 2R^2 P_r S_{n_L} B_d. \quad (3.27)$$

The shot noise has a variance of

$$\sigma_{sh}^2 = 2eR(P_{LO} + P_r + 2S_{n_s} \Delta f_{o,s} + 2S_{n_L} \Delta f_{o,L}) B_d \quad (3.28)$$

for LO, signal, and spontaneous induced shot noise.

For both heterodyne or homodyne system, the SNR of the signal is

$$\rho_s = \frac{P_r}{S_{n_s} B_d + \frac{P_r}{P_{LO}} S_{n_L} B_d + \frac{\hbar\omega_c}{\eta} \left(1 + \frac{P_r}{P_{LO}}\right) B_d}, \quad (3.29)$$

when the shot noise of spontaneous emission and the beating of spontaneous emission with shot noise are ignored.

The LO spontaneous emission noise usually comes from a single amplifier with spectral density of

$$S_{n_L} = (G_L - 1)n_{spL}\hbar\omega_{LO} \quad (3.30)$$

where G_L and n_{spL} are the gain and spontaneous emission factor of the LO amplifier.

The spontaneous emission noise of S_{n_s} together with the received signal is induced by a chain of optical amplifiers in the fiber link. Assume N_A identical fiber link with loss of $1/G_s$, equal to the gain of the N_A identical optical amplifiers, the first optical amplifier has a spontaneous emission noise of

$$(G_s - 1)n_{sp_s}\hbar\omega_c. \quad (3.31)$$

where n_{sp_s} is the spontaneous emission factor of the optical amplifier at the fiber link. The above spontaneous emission losses a factor of $1/G_s$ at the fiber link, and is amplified by G_s by the second optical amplifier. The second optical amplifiers also add a spontaneous emission the same as Eq. (3.31) to the optical signal. After N_A fiber span, we obtain

$$S_{n_s} = N_A(G_s - 1)n_{sp_s}\hbar\omega_c. \quad (3.32)$$

The noise figure of optical amplifier is approximated equal to $2n_{sp_s}$. The spontaneous emission of Eq. (3.32) can be expressed using the noise figure of the optical amplifier.

Shot noise limited systems

A heterodyne system without optical amplifiers is limited by the shot noise with $n_s(t) = 0$ and $n_L(t) = 0$, the signal power is that of Eq. (3.25) and the noise variance is that of Eq. (3.28). The SNR of a heterodyne system becomes

$$\rho_s = \frac{RP_r}{eB_d} \quad (3.33)$$

For binary signal, if the number of photons per bit is N_s , $P_r = N_s\hbar\omega_c B_d$. For multilevel signal, N_s is the number of photons per symbol. With the responsivity defined by Eq. (3.6), we get

$$\rho_s = \eta N_s. \quad (3.34)$$

In homodyne system, the power twice that of Eq. (3.25) but the shot-noise remain the same as that of Eq. (3.28), the SNR is

$$\rho_s = 2\eta N_s. \quad (3.35)$$

In the quantum limit with $\eta = 1$, the quantum limited SNR is N_s and $2N_s$ for heterodyne and homodyne system, respectively.

Amplifier noise limited systems

With the condition of Eq. (3.12), the SNR after the balanced receiver for heterodyne system with $\omega_{IF} \neq 0$ is

$$\rho_s = \frac{P_r}{S_{n_s} B_d}. \quad (3.36)$$

The SNR of Eq. (3.36) has a very clear physical meaning of the signal P_r over the optical noise within a bandwidth of B_d in a single polarization. As the spontaneous emission has a spectral density of S_{n_s} , the noise power per polarization is $S_{n_s} B_d$. In a RF system, with proper filtering, mixing by upconversion or downconversion does not change the SNR. We may use the SNR in optical domain, before the downconversion by balanced receiver, as the SNR in the receiver. Of course, the definition of the SNR of Eq. (3.36) ignored the amplifier noise in orthogonal polarization. In the photocurrent of Eq. (3.21), the optical amplifier noise from orthogonal polarization does not affect the system.

For a received power of $P_r = G_s N_s \hbar \omega_c B_d$, we get

$$\rho_s = \frac{N_s}{N_A n_{\text{sps}}} \frac{G_s}{G_s - 1} \approx \frac{N_s}{N_A n_{\text{sps}}} \quad (3.37)$$

Comparing with Eq. (3.34), the SNR is degraded by the factor of $N n_{\text{sps}}$. The SNR of Eq. (3.37) is valid for both homodyne and heterodyne systems. For heterodyne systems, the condition of Eq. (3.12) must be satisfied.

We may define $n_{\text{eq}} = N_A n_{\text{sps}} (G_s - 1) / G_s = \frac{1}{2} N_A F_n$ for N_A identical optical amplifiers where F_n is the noise figure of each optical amplifiers. With the equivalent spontaneous emission factor of n_{eq} , the spectrum density of Eq. (3.32) becomes

$$S_{n_s} = (G_s - 1) n_{\text{eq}} \hbar \omega_c. \quad (3.38)$$

and the SNR is

$$\rho_s = \frac{N_s}{n_{\text{eq}}}. \quad (3.39)$$

If the N optical amplifiers are not the same with different gain and noise figure, the equivalent spontaneous emission factor is

$$n_{\text{eq}} = \sum_{k=1}^{N_A} \frac{P_{\text{in}N}}{P_{\text{in}k}} \frac{G_k - 1}{G_k} n_{\text{sps}k}, \quad (3.40)$$

where G_k , $k = 1, \dots, N_A$, are the gain of each optical amplifier, $P_{\text{in}k}$, $k = 1, \dots, N_A$, are the input power of each optical amplifier, and $n_{\text{sps}k}$ are the spontaneous emission factor of each optical amplifier. If all amplifiers are identical with gain of $G_k = G_s$, we get $n_{\text{eq}} = N_A n_{\text{sps}} (G_s - 1) / G_s$.

The SNR of Eq. (3.39) is the same as the optical SNR defined over a bandwidth of B_d for a single polarization of

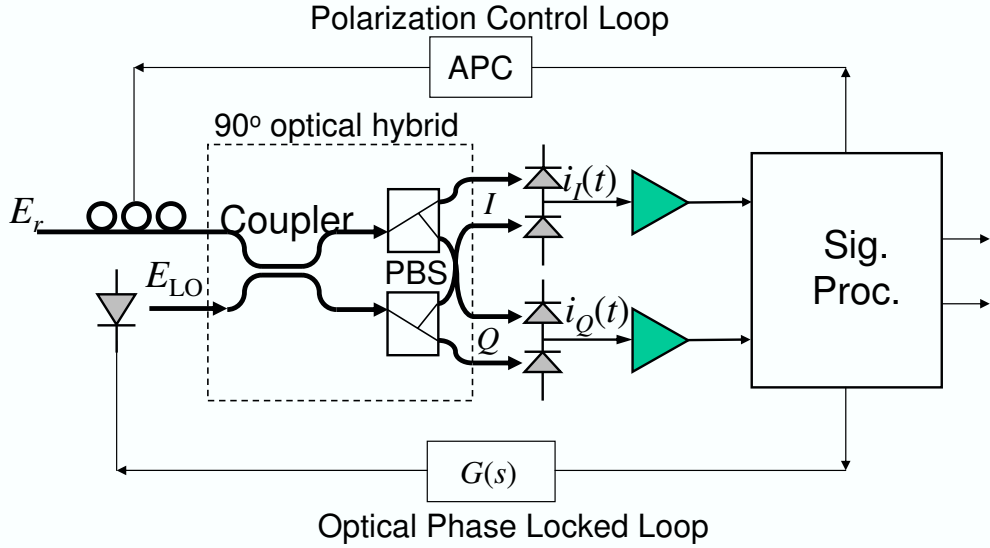


Figure 3.4: A quadrature homodyne receiver.

$$\frac{P_r}{S_{n_s} B_d} = \frac{N_s}{n_{\text{eq}}}. \quad (3.41)$$

In the quantum of a single optical amplifier of $N_A = 1$ and $F_n = 2$ (or 3 dB), $n_{\text{eq}} = 1$, the quantum limited SNR is equal to the number of photon per bit of N_s , the same as that of shot-noise limited heterodyne system.

The SNR of Eq. (3.39) is equal to

$$\rho_s = \text{SNR}_o, s \frac{\Delta f_{o,s}}{2B_d}, \quad (3.42)$$

where the factor of 2 is for two polarizations in most optical SNR measurement.

If no optical filter is used or the optical filter has a wide bandwidth to invalidate the condition of Eq. (3.12), the amplifier-limited SNR for heterodyne receiver is

$$\rho_s = \frac{N_s}{2n_{\text{eq}}}. \quad (3.43)$$

In later section, we always assume a SNR of Eq. (3.39) for heterodyne receiver. With a balanced receiver, the performance of a system depends solely on the SNR. Both heterodyne and homodyne systems have the same performance if the SNR of the system is the same.

Balanced receiver for coherent optical communications was first analyzed in detail by Yuen and Chan (1983) and Abbas et al. (1985) to suppress the LO noise and to gain 3-dB more signal power. Without LO noise and ignored thermal noise, the performance of balanced receiver should be the same as that of a single branch receiver.

3.1.3 Quadrature Receiver

Figure 3.4 shows a quadrature receiver to receive the in- and quadrature-phase components of the optical signal. The quadrature receiver based on a 90° optical hybrid and two balanced receivers. Although a single branch receiver of Fig. 3.1 can be used in Fig. 3.4, a balanced receiver has better perform, especially in the presence of LO laser noise.

The 90° optical hybrid composites of a 3-dB coupler and two polarization beam splitters (PBS). Using the two PBS as the reference polarization, the received signal must be controlled to be linearly

polarization with a direction 45° apart with the PBS reference directions. The noiseless received signal is

$$E_r = \frac{1}{\sqrt{2}}(\mathbf{x} + \mathbf{y})A_s(t)e^{j\phi_s(t)+j\omega_c t}. \quad (3.44)$$

The LO laser must be circular polarized with

$$E_{\text{LO}} = \frac{1}{\sqrt{2}}(\mathbf{x} + e^{j\pi/2}\mathbf{y})A_L e^{j\omega_{\text{LO}}t}. \quad (3.45)$$

At the output of the 3-dB coupler, the two electric fields are

$$\begin{aligned} E_1 &= \frac{1}{\sqrt{2}}(E_r + E_{\text{LO}}) \\ &= \frac{\mathbf{x}}{2} \underbrace{\left[A_s(t)e^{j\phi_s(t)+j\omega_c t} + A_L e^{j\omega_{\text{LO}}t} \right]}_{0^\circ} \\ &\quad + \frac{\mathbf{y}}{2} \underbrace{\left[A_s(t)e^{j\phi_s(t)+j\omega_c t} + A_L e^{j\omega_{\text{LO}}t+j\pi/2} \right]}_{90^\circ}, \end{aligned} \quad (3.46)$$

and

$$\begin{aligned} E_2 &= \frac{1}{\sqrt{2}}(E_r - E_{\text{LO}}) \\ &= \frac{\mathbf{x}}{2} \underbrace{\left[A_s(t)e^{j\phi_s(t)+j\omega_c t} - A_L e^{j\omega_{\text{LO}}t} \right]}_{180^\circ} \\ &\quad + \frac{\mathbf{y}}{2} \underbrace{\left[A_s(t)e^{j\phi_s(t)+j\omega_c t} - A_L e^{j\omega_{\text{LO}}t+j\pi/2} \right]}_{270^\circ}. \end{aligned} \quad (3.47)$$

The upper balanced receiver combines the photocurrents corresponding to both 0° and 180° , the received photocurrent is

$$\begin{aligned} i_I(t) &= \frac{R}{4} \left| A_s(t)e^{j\phi_s(t)+j\omega_c t} + A_L e^{j\omega_{\text{LO}}t} \right|^2 - \frac{R}{4} \left| A_s(t)e^{j\phi_s(t)+j\omega_c t} - A_L e^{j\omega_{\text{LO}}t} \right|^2 \\ &= RA_s(t)A_L \cos[\omega_{\text{IF}}t + \phi_s(t)]. \end{aligned} \quad (3.48)$$

The lower balanced receiver combines the photocurrents corresponding to both 90° and 270° , the received photocurrent is

$$\begin{aligned} i_Q(t) &= \frac{R}{4} \left| A_s(t)e^{j\phi_s(t)+j\omega_c t} + A_L e^{j\omega_{\text{LO}}t+j\pi/2} \right|^2 \\ &\quad - \frac{R}{4} \left| A_s(t)e^{j\phi_s(t)+j\omega_c t} - A_L e^{j\omega_{\text{LO}}t+j\pi/2} \right|^2 \\ &= RA_s(t)A_L \sin[\omega_{\text{IF}}t + \phi_s(t)]. \end{aligned} \quad (3.49)$$

In both photocurrents of Eq. (3.48) and Eq. (3.49), the IF frequency of ω_{IF} is not equal to zero for a more general application for a quadrature receiver.

Mathematically, a 2×2 90° optical hybrid has an input and output relationship of

$$S = \frac{1}{2} \begin{bmatrix} 1 & 1 \\ 1 & j \end{bmatrix}. \quad (3.50)$$

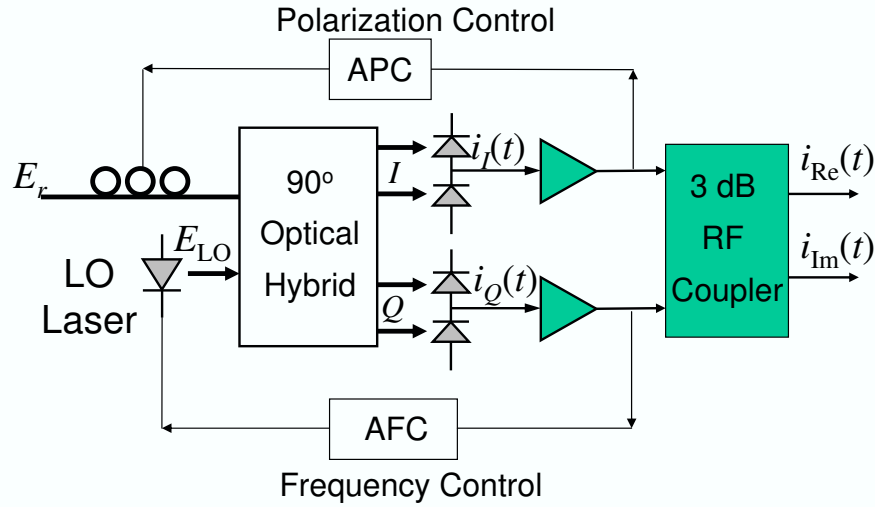


Figure 3.5: A heterodyne image-rejection receiver.

and a 2×4 90° optical hybrid has an input and output relationship of

$$S = \frac{1}{2} \begin{bmatrix} 1 & 1 \\ 1 & j \\ 1 & -1 \\ 1 & -j \end{bmatrix}. \quad (3.51)$$

For a homodyne receiver with a phase-locked loop Fig. 3.4, $\omega_{IF} = 0$ and $i_I(t)$ gives the in-phase component proportional to $A_s(t) \cos \phi_s(t)$ and $i_Q(t)$ provides the quadrature-phase component proportional to $A_s(t) \sin \phi_s(t)$. The quadrature homodyne receiver can be used as the receiver of either M -ary PSK or quadrature-amplitude modulation (QAM) signals.

In the quadrature receiver of Fig. 3.4, the shot-noise limited SNR is the same as that in Eq. (3.35) and the amplifier-noise limited SNR is that of Eq. (3.39). The noises in the in- and quadrature-phase components are independent of each other. The SNR for the photocurrents of Eq. (3.48) and Eq. (3.49) is identical.

For a heterodyne receiver with $\omega_{IF} \neq 0$, $i_I(t)$ and $i_Q(t)$ are quadrature components with a phase difference of 90° . However, in heterodyne receiver, it may be more convenient to use microwave techniques to provide both in- and quadrature-phase components. Of course, as shown later, a heterodyne quadrature receiver similar to Fig. 3.4 can be used to provide image-rejection.

Simultaneous in- and quadrature-phase detection was first used to simultaneously measure phase and amplitude of an electric field (Walker and Carroll, 1984). The first application to coherent optical communication was by Hodgkinson et al. (1985). The 90° optical hybrid of Fig. 3.4 is designed according to Kazovsky et al. (1987). Other implementations of 90° optical hybrid were proposed by Delavaux et al. (1990), Delavaux and Riggs (1990), Hoffman et al. (1989), Langenhorst et al. (1991). As shown later, both image-rejection and phase-diversity receivers are based on the quadrature receiver of Fig. 3.4.

3.1.4 Image-Rejection Heterodyne Receiver

In a densely space coherent wavelength-division-multiplexed (WDM) systems, the most important issues is to improve the spectral efficiency by allotting more channels within the passband of the system. In the heterodyne receiver with $\omega_{IF} \neq 0$ in both Fig. 3.1 and Fig. 3.3, the signal at both ω_{c1} and ω_{c2} fall to the same IF band if $\omega_{IF} = \omega_{c1} - \omega_{LO} = \omega_{LO} - \omega_{c2}$. In a regular balanced heterodyne receiver of Fig. 3.3, a large guard-band about $2\omega_{IF}$ is required such that the negative or image band signals do not interfere with each other. The requirement of large guard-band limits the spectral efficiency of the systems.

Figure 3.5 shows a image-rejection receiver with an optical front-end similar to the quadrature receiver of Fig. 3.4 with an 90° optical hybrid and two balanced receivers. The image-rejection receiver of Fig. 3.5 is for heterodyne with $\omega_{IF} > 0$. Assume that there are two signals at ω_{c1} and ω_{c2} with a relation of

$$\omega_{IF} = \omega_{c1} - \omega_{LO} = \omega_{LO} - \omega_{c2}. \quad (3.52)$$

If the two signals are $E_{c1}(t) = A_{s1}(t)e^{j\omega_{c1}t + j\phi_{s1}(t)}$ and $E_{c2}(t) = A_{s2}(t)e^{j\omega_{c2}t + j\phi_{s2}(t)}$, similar to Eq. (3.48) and Eq. (3.49) and without going into details, we obtain two photocurrents of

$$\begin{aligned} i_I(t) = & RA_{s1}(t)A_L \cos[(\omega_{c1} - \omega_{LO})t + \phi_{s1}(t)] \\ & + RA_{s2}(t)A_L \cos[(\omega_{LO} - \omega_{c2})t - \phi_{s2}(t)], \end{aligned} \quad (3.53)$$

and

$$\begin{aligned} i_Q(t) = & RA_{s1}(t)A_L \sin[(\omega_{c1} - \omega_{LO})t + \phi_{s1}(t)] \\ & - RA_{s2}(t)A_L \sin[(\omega_{LO} - \omega_{c2})t - \phi_{s2}(t)]. \end{aligned} \quad (3.54)$$

After the 90° microwave hybrid², we obtain

$$i_{Re}(t) = \sqrt{2}RA_{s1}(t)A_L \cos[(\omega_{c1} - \omega_{LO})t + \phi_{s1}(t)], \quad (3.55)$$

$$i_{Im}(t) = \sqrt{2}RA_{s2}(t)A_L \cos[(\omega_{LO} - \omega_{c2})t - \phi_{s2}(t)] \quad (3.56)$$

for the real and image frequency band, respectively.

In an image-rejection heterodyne receiver of Fig. 3.5, even without an optical filter to reject the image-band spontaneous emission, the amplifier-noise limited SNR is $\rho_s = N_s/(N_A n_{sp})$ from Eq. (3.39). Not only reject the signal from the image band, the image-rejection receiver also reject the noise from the image band.

In another application of the image-rejection of Fig. 3.5, the LO laser can have a frequency between two WDM channels. The real and image band can be processed to receive the WDM channels having larger or smaller frequency than the LO laser.

Heterodyne image-rejection receiver was proposed by Darcie and Glance (1986), Glance (1986), Westphal and Strebel (1988) and used by Chikama et al. (1990), Lachs et al. (1990) for WDM systems. Even without optical filter, as proposed by Glance et al. (1988), Walker et al. (1990) and Jørgensen et al. (1992) showed that the SNR is improved by 3-dB using image rejection receiver.

3.1.5 SNR of Basic Coherent Receivers

Table 3.1 summaries the SNR of system having difference receiver structures. Single-branch receiver is more likely to be limited by the noise from LO laser.

For system limited by amplifier noise, without optical filter, heterodyne receiver is 3-dB worse than homodyne receiver. Image-rejection eliminates the noise at the imagine frequency band for system even without optical filtering. Homodyne and heterodyne receiver has the same SNR for both cases of having image-rejection or optical filtering. The optical filter of heterodyne system must have an optical bandwidth for the relationship of Eq. (3.12).

²The transfer matrix must be

$$S = \frac{1}{\sqrt{2}} \begin{bmatrix} 1 & j \\ 1 & -j \end{bmatrix}$$

with a 90° shift from Eq. (3.1). The transfer matrix is called 90° microwave hybrid but similar matrix as 180° optical hybrid.

Table 3.1: Comparison of the SNR of Different Receiver Structure

Receiver Types	Shot Noise Limited	Amplifier Noise Limited
Single-branch heterodyne w/ optical filter [†]	ηN_s	$\frac{N_s}{n_{\text{eq}}}$
Single-branch heterodyne w/o optical filter [†]	ηN_s	$\frac{2n_{\text{eq}}}{N_s}$
Single-branch homodyne [†]	$2\eta N_s$	$\frac{N_s}{n_{\text{eq}}}$
Balanced received heterodyne w/ optical filter	ηN_s	$\frac{n_{\text{eq}}}{N_s}$
Balanced received heterodyne w/o optical filter	ηN_s	$\frac{2n_{\text{eq}}}{N_s}$
Balanced homodyne	$2\eta N_s$	$\frac{N_s}{n_{\text{eq}}}$
Quadrature homodyne	$2\eta N_s$	$\frac{N_s}{n_{\text{eq}}}$
Image-rejection heterodyne receiver	ηN_s	$\frac{N_s}{n_{\text{eq}}}$

[†] Single-branch receiver is more likely to be limited by LO noise.

For system limited by shot-noise, the performance of heterodyne receiver is always 3-dB worse than homodyne receiver. This 3-dB difference was observed by all standard textbooks (Agrawal, 2002, Betti et al., 1995, Okoshi and Kikuchi, 1988).

In later parts of this book, system performance is analyzed based on the representation of a received signal of

$$r(t) = A_s(t) \cos[\omega_{\text{IF}} + \phi_s(t)] + n(t) \quad (3.57)$$

with the SNR coming from Table 3.1. The noise in the receiver is considered to be within the narrow receiver bandwidth of a coherent receiver and with a band-pass representation of

$$n(t) = n_1(t) \cos \omega_{\text{IF}} t - n_2(t) \sin \omega_{\text{IF}} t \quad (3.58)$$

with

$$E\{n^2(t)\} = E\{n_1^2(t)\} = E\{n_2^2(t)\} = \sigma_n^2. \quad (3.59)$$

As discussed earlier, a quantum-limited system has the limited of $\eta = 1$ and $n_{\text{eq}} = 1$. The quantum-limited SNR is equal to the number of photons per bit (or per symbol) for heterodyne system limited by either shot or amplifier noise.

3.2 Performance of Synchronous Detection Receiver

When an optical phase-locked loop (PLL) is used to track the phase of the LO laser for homodyne systems or a microwave PLL is used to track the phase of a LO oscillator for heterodyne systems, the system is called a coherent system according to the terminology of conventional digital communications (Proakis, 2000). In coherent optical communications, system with phase tracking is called synchronous detection system. This section calculates the error probability of synchronous detection system. With the same SNR of ρ_s , homodyne and heterodyne system has the same performance. This section considers only heterodyne systems with balanced receiver.

3.2.1 Amplitude-Shift Keying

When the light is ASK modulated, the signal current of Eq. (3.24) in a heterodyne receiver can be expressed as

$$s_1(t) = A \cos \omega_{\text{IF}} t, \quad (3.60)$$

$$s_2(t) = 0. \quad (3.61)$$

The above ASK signal can be received by the heterodyne receiver of Fig. 1.3(b).

The overall signal is

$$r(t) = s(t) + n(t) = \begin{cases} [A + n_1(t)] \cos \omega_{\text{IF}} t - n_2(t) \sin \omega_{\text{IF}} t & \text{for } s_1(t) \\ n_1(t) \cos \omega_{\text{IF}} t - n_2(t) \sin \omega_{\text{IF}} t & \text{for } s_2(t) \end{cases}. \quad (3.62)$$

With threshold of $\frac{1}{2}A$, the error probability is

$$p_e = \frac{1}{2} \int_{-\infty}^{\frac{A}{2}} p_1(x) dx + \frac{1}{2} \int_{\frac{A}{2}}^{+\infty} p_2(x) dx \quad (3.63)$$

where

$$p_1(x) = \frac{1}{\sqrt{2\pi}\sigma_n} e^{-\frac{(x-A)^2}{2\sigma_n^2}}, \quad (3.64)$$

$$p_2(x) = \frac{1}{\sqrt{2\pi}\sigma_n} e^{-\frac{x^2}{2\sigma_n^2}}. \quad (3.65)$$

We obtain

$$p_e = \frac{1}{2} \text{erfc} \left(\frac{A}{2\sqrt{2}\sigma_n} \right) \quad (3.66)$$

$$= \frac{1}{2} \text{erfc} \left(\sqrt{\frac{\rho_s}{2}} \right) \quad (3.67)$$

where the SNR is

$$\rho_s = \frac{A^2/4}{\sigma_n^2}. \quad (3.68)$$

with signal power equal to $\frac{1}{2} \frac{A^2}{2} + 0 = \frac{A^2}{4}$.

To achieve an error probability of 10^{-9} , a SNR of $\rho_s = 36$ (15.6 dB). The quantum-limited ASK system require 36 photons per bit.

3.2.2 Phase-Shift Keying

When the light is PSK modulated, the signal current of Eq. (3.24) in a heterodyne receiver can be expressed as

$$s_1(t) = A \cos \omega_{\text{IF}} t, \quad (3.69)$$

$$s_2(t) = -A \cos \omega_{\text{IF}} t. \quad (3.70)$$

The above ASK signal can be received by the heterodyne receiver of Fig. 1.3(b). The overall received signal is

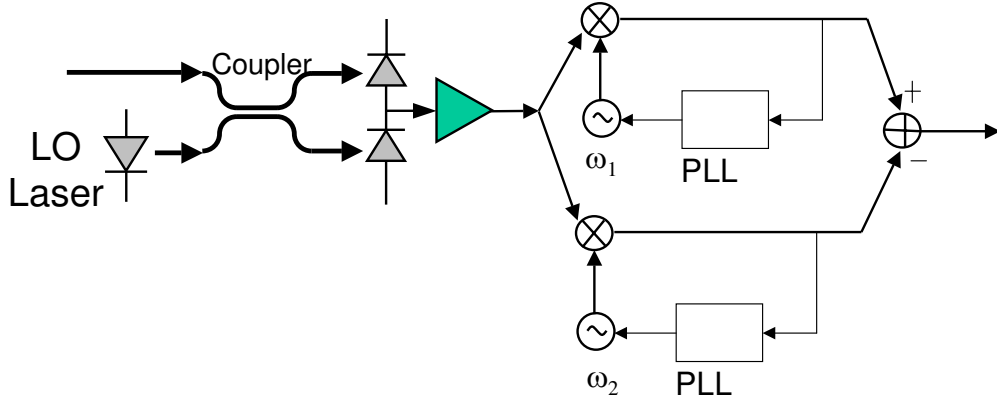


Figure 3.6: A heterodyne synchronous receiver for FSK signal.

$$r(t) = s(t) + n(t) = \begin{cases} [A + n_1(t)] \cos \omega_{IF}t - n_2(t) \sin \omega_{IF}t & \text{for } s_1(t) \\ [-A + n_1(t)] \cos \omega_{IF}t - n_2(t) \sin \omega_{IF}t & \text{for } s_2(t) \end{cases} \quad (3.71)$$

With threshold of zero, the error probability is

$$p_e = \frac{1}{2} \int_{-\infty}^0 p_1(x) dx + \frac{1}{2} \int_0^{+\infty} p_2(x) dx \quad (3.72)$$

where

$$p_1(x) = \frac{1}{\sqrt{2\pi}\sigma_n} e^{-\frac{(x-A)^2}{2\sigma_n^2}}, \quad (3.73)$$

$$p_2(x) = \frac{1}{\sqrt{2\pi}\sigma_n} e^{-\frac{(x+A)^2}{2\sigma_n^2}}. \quad (3.74)$$

We obtain

$$p_e = \frac{1}{2} \operatorname{erfc} \left(\frac{A}{\sqrt{2}\sigma_n} \right) \quad (3.75)$$

$$= \frac{1}{2} \operatorname{erfc} (\sqrt{\rho_s}) \quad (3.76)$$

where the SNR is

$$\rho_s = \frac{A^2/2}{\sigma_n^2}. \quad (3.77)$$

To achieve an error probability of 10^{-9} , a SNR of $\rho_s = 18$ (12.5 dB). The quantum-limited PSK system require 18 photons per bit.

3.2.3 Frequency-Shift Keying

When the light is FSK modulated, the signal current of Eq. (3.24) in a heterodyne receiver can be expressed as

$$s_1(t) = A \cos \omega_1 t \quad (3.78)$$

$$s_2(t) = A \cos \omega_2 t \quad (3.79)$$

where ω_1 and ω_2 are two orthogonal frequencies where

$$\int_0^T s_1(t)s_2(t)dt = 0 \quad (3.80)$$

where T is the symbol interval. The two frequencies should be separated by $\omega_1 - \omega_2 = k\pi/T$, $k = \pm 1, \pm 2, \dots$. In a synchronous detected heterodyne FSK signal, two microwave PLL are required to phase locking into either ω_1 and ω_2 . Equivalently, two matched filters can be used with filter response corresponds to $s_1(t)$ and $s_2(t)$, respectively.

A FSK signal can be received by the receiver of Fig. 3.6 with two PLLs locking into the angular frequency of ω_1 and ω_2 . The difference of the two outputs of Fig. 3.6 decides whether $s_1(t)$ or $s_2(t)$ is transmitted.

With the orthogonal condition, the overall signal is

$$r(t) = s(t) + n(t) = \begin{cases} [A + n_{11}(t)] \cos \omega_1 t - n_{12}(t) \sin \omega_1 t & \text{for } s_1(t) \\ [A + n_{21}(t)] \cos \omega_2 t - n_{22}(t) \sin \omega_2 t & \text{for } s_2(t) \end{cases} \quad (3.81)$$

where $n_{11}(t)$, $n_{21}(t)$, $n_{12}(t)$, and $n_{22}(t)$ are independent of each other with the same variance of σ_n^2 . When $s_1(t)$ is transmitted, the correct decision is $A + n_{11}(t) > n_{21}(t)$ or $A + n_{11}(t) - n_{21}(t) > 0$. The noise of $n_{11}(t) - n_{21}(t)$ has a variance of $2\sigma_n^2$. The error probability is the same as that of PSK signal but with a noise variance of $2\sigma_n^2$, we obtain

$$p_e = \frac{1}{2} \operatorname{erfc} \left(\frac{A}{2\sigma_n} \right) \quad (3.82)$$

$$= \frac{1}{2} \operatorname{erfc} \left(\sqrt{\frac{\rho_s}{2}} \right) \quad (3.83)$$

where the SNR is

$$\rho_s = \frac{A^2/2}{\sigma_n^2}. \quad (3.84)$$

A FSK signal has the same performance as ASK modulated signal. The same as ASK signal, to achieve an error probability of 10^{-9} , a SNR of $\rho_s = 36$ (15.6 dB). The quantum-limited FSK system require 36 photons per bit.

The performance of synchronous receiver, the same as digital signal with a matched filter provided by phase tracking, is analyzed in Proakis (2000) or the early paper of Yamamoto (1980).

3.3 Performance of Asynchronous Coherent Receiver

All of ASK, DPSK, and FSK can be detected without phase tracking. The detection is based on the comparison of the power or envelope of the signal. This type of detection is called non-coherent detection in conventional digital communications (Proakis, 2000) and asynchronous receiver in optical communications. In this section, we consider asynchronous heterodyne receiver with signal processing by microwave circuit in the IF.

3.3.1 Envelope Detection of Heterodyne ASK Receiver

Figure 3.7 shows the receiver for envelope detection of heterodyne ASK signals. The signal first passing through a band-pass filter (BPF) to limited the amount of noise. After the BPF, the signal is the same as that of Eq. (3.62). The signal of Eq. (3.62) is squared, low-pass filtered (LPF), square-rooted, to obtain the envelope of

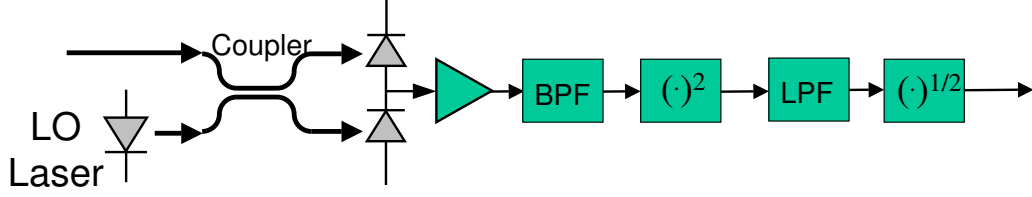


Figure 3.7: A heterodyne asynchronous receiver for ASK signal.

$$r_d(t) = \begin{cases} \sqrt{[A + n_1(t)]^2 + n_2^2(t)} & \text{for } s_1(t) \\ \sqrt{n_1^2(t) + n_2^2(t)} & \text{for } s_2(t) \end{cases}. \quad (3.85)$$

with p.d.f. of

$$p_1(r) = \frac{r}{\sigma_n^2} I_0\left(\frac{rA}{\sigma_n^2}\right) \exp\left(-\frac{r^2 + A^2}{2\sigma_n^2}\right), \quad (3.86)$$

$$p_2(r) = \frac{r}{\sigma_n^2} \exp\left(-\frac{r^2}{2\sigma_n^2}\right), \quad (3.87)$$

where $I_0(\cdot)$ is the zeroth-order modified Bessel function of the first kind. In the decision random variable of Eq. (3.85), some constant factors relate to gain and loss of the squarer, LPF, and the square-root components are ignored. The envelope of Eq. (3.85) is the same as the amplitude of the signal. The error probability of the system is

$$p_e = \frac{1}{2} \left[1 - \int_{r_{\text{th}}}^{\infty} p_1(r) dr \right] + \frac{1}{2} \int_{r_{\text{th}}}^{\infty} p_2(r) dr, \quad (3.88)$$

where r_{th} is the threshold. Using the Marcum's Q -function defined by Eq. (200) from Appendix 3.8, we obtain

$$p_e = \frac{1}{2} \left[1 - Q\left(\frac{A}{\sigma_n}, \frac{r_{\text{th}}}{\sigma_n}\right) \right] + \frac{1}{2} \exp\left(-\frac{r_{\text{th}}^2}{2\sigma_n^2}\right). \quad (3.89)$$

The optimal threshold can be found by $dp_e/dr_{\text{th}} = 0$ as

$$I_0\left(\frac{Ar_{\text{th}}}{\sigma_n^2}\right) \exp\left(-\frac{A^2}{2\sigma_n^2}\right) = 1. \quad (3.90)$$

The optimal threshold is difficult to find analytically, we may use the approximation of $r_{\text{th}} = A/2$. With this threshold, the second term of Eq. (3.89) is larger than the first term and the error probability is approximately equal to (Ryu, 1995)

$$\begin{aligned} p_e &\approx \frac{1}{2} \exp\left(-\frac{A^2}{8\sigma_n^2}\right) \\ &= \frac{1}{2} \exp\left(-\frac{\rho_s}{2}\right). \end{aligned} \quad (3.91)$$

Based on the approximation of Eq. (3.91), the required SNR for an error probability of 10^{-9} is $\rho_s = 40$ (16 dB). The quantum limit is 40 photons per bit.

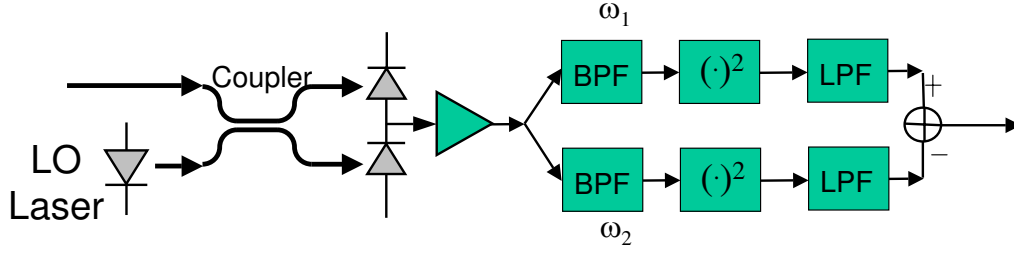


Figure 3.8: A heterodyne asynchronous receiver for FSK signal.

3.3.2 Dual-Filter Detection of FSK Signal

Figure 3.8 shows an asynchronous heterodyne receiver for FSK signal based on two BPF's matched to the FSK signals of $s_1(t)$ and $s_2(t)$ having center angular frequency of ω_1 and ω_2 , respectively. Based on Eq. (3.81), when $s_1(t)$ is transmitted, the received signal at the first filter centered at ω_1 is the similar to that of Eq. (3.85). Although not necessary, an square root is assumed for the signal of Fig. 3.8. When $s_1(t)$ is transmitted, we obtain

$$r_1(t) = \sqrt{[A + n_{11}(t)]^2 + n_{12}^2(t)}, \quad (3.92)$$

and

$$r_2(t) = \sqrt{n_{21}^2(t) + n_{22}^2(t)} \quad (3.93)$$

with p.d.f. of

$$p_1(r_1) = \frac{r_1}{\sigma_n^2} I_0 \left(\frac{r_1 A}{\sigma_n^2} \right) \exp \left(-\frac{r_1^2 + A^2}{2\sigma_n^2} \right), \quad (3.94)$$

$$p_2(r_2) = \frac{r_2}{\sigma_n^2} \exp \left(-\frac{r_2^2}{2\sigma_n^2} \right). \quad (3.95)$$

Bit error occurs when $r_1 < r_2$, or

$$p_e = \Pr\{r_1 < r_2\} = \Pr\{r_1^2 < r_2^2\}. \quad (3.96)$$

From Eq. (3.96), a square-root is not required in Fig. 3.8. The error probability is

$$\begin{aligned} p_e &= \int_{r_1}^{\infty} p_1(r_1) \int_{r_1}^{\infty} p_2(r_2) dr_2 dr_1 \\ &= \int_0^{\infty} \frac{r_1}{\sigma_n^2} I_0 \left(\frac{r_1 A}{\sigma_n^2} \right) \exp \left(-\frac{2r_1^2 + A^2}{2\sigma_n^2} \right) dr_1 \\ &= \frac{1}{2} \exp \left(-\frac{A^2}{4\sigma_n^2} \right) \int_0^{\infty} \frac{2r_1}{\sigma_n^2} I_0 \left(\frac{2r_1 A}{2\sigma_n^2} \right) \exp \left(-\frac{4r_1^2 + A^2}{4\sigma_n^2} \right) dr_1 \\ &= \frac{1}{2} \exp \left(-\frac{A^2}{4\sigma_n^2} \right) \\ &= \frac{1}{2} \exp \left(-\frac{\rho_s}{2} \right). \end{aligned} \quad (3.97)$$

The above error probability is valid only if the two signals are orthogonal. The performance of FSK signal is the same as that of ASK signal.

A FSK signal can detect based on a single filter. The signal after the filter is similar to an ASK signal. The performance of FSK signal with a single filter is similar to that of ASK signal with an error probability of $p_e = \frac{1}{2} \exp(-\frac{\rho_s}{4})$. While an ASK signal has no power at the “0” level, the power of FSK signal is the same at both “0” and “1” levels. The performance of FSK signal is 3-dB worse than the equivalent ASK signal. Intuitively, using a single filter, the FSK signal is also 3-dB worse than a dual-filter receiver.

3.3.3 DPSK Heterodyne Differential Detection

In a heterodyne DPSK system, the received signal is

$$r(t) = \Re\{[Ae^{j\phi_s(t)} + n(t)]e^{j\omega_{IF}t}\} \quad (3.98)$$

or

$$r(t) = \Re\{\tilde{r}(t)e^{j\omega_{IF}t}\} \quad (3.99)$$

where $\tilde{r}(t) = Ae^{j\phi_s(t)} + \tilde{n}(t)$ is the baseband representation of the IF signal with $\tilde{n}(t) = n_1(t) + jn_2(t)$. The DPSK signal is demodulated by delay-and-multiplier circuits of Fig. 1.4(b). If $\tilde{r}(t)$ is expressed as $\tilde{r} = \tilde{A}_1(t)e^{j\tilde{\phi}_1(t)}$, the demodulated signal after a low-pass filter is

$$\begin{aligned} r_d(t) &= \tilde{A}_1(t)\tilde{A}_1(t-T) \cos[\tilde{\phi}_1(t) - \tilde{\phi}_1(t-T)] \\ &= \Re\{\tilde{r}(t)\tilde{r}^*(t-T)\}. \end{aligned} \quad (3.100)$$

In addition to the transmitted phase of $\phi_s(t)$, $\tilde{\phi}_1(t)$ includes the phase due to $\tilde{n}(t)$. The delay of τ must be approximated equal to T and $\omega_{IF}\tau$ must be integer multiple of 2π .

It is obvious that

$$r_d(t) = \left| \frac{\tilde{r}(t) + \tilde{r}(t-T)}{2} \right| - \left| \frac{\tilde{r}(t) - \tilde{r}(t-T)}{2} \right| \quad (3.101)$$

Because $\tilde{r}(t) + \tilde{r}(t-T)$ and $\tilde{r}(t) - \tilde{r}(t-T)$ are independent of each other, the error probability is similar to Eq. (3.96) with

$$p_e = \Pr\{r_1 < r_2\} = \Pr\{r_1^2 < r_2^2\} = \Pr\{r_d < 0\} \quad (3.102)$$

with r_1^2 as the first term of Eq. (3.101) that is the square of a Gaussian random variable with mean of A and variance of σ_n^2 and r_2^2 as the second term of Eq. (3.101) is the square of a Gaussian random variable with zero mean and variance of σ_n^2 . The error probability is the same as that for FSK signal of Eq. (3.83) with SNR of $\frac{1}{2}A^2/\sigma_n^2$, i.e.,

$$\begin{aligned} p_e &= \frac{1}{2} \exp\left(-\frac{A^2}{2\sigma_n^2}\right) \\ &= \frac{1}{2} \exp(-\rho_s). \end{aligned} \quad (3.103)$$

The error probability of Eq. (3.103) was derived by Cahn (1959) using approximation. DPSK signal was analyzed the same as orthogonal signal by Stein (1964). Using two time intervals, the performance of DPSK signal is 3-dB better than that of FSK signal. In Eq. (3.101), although the mean of the signal when two consecutive time intervals using the same phases is the same as that of FSK signal, the noise variance is reduced by half because the noise is averaged of that from two time intervals.

The required SNR for an error probability of 10^{-9} is $\rho_s = 20$ (13 dB) for DPSK signal. The quantum limit is 20 photons per bit.

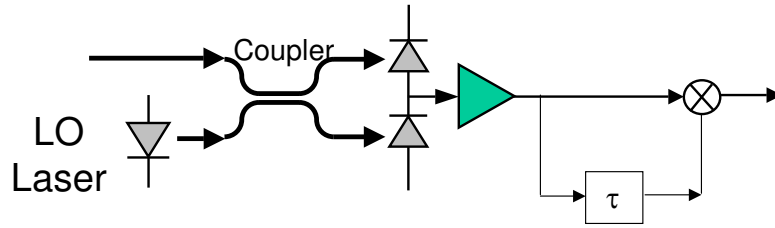


Figure 3.9: A heterodyne asynchronous receiver for CPFSK signal based on delay-and-multiplier circuits.

3.3.4 CPFSK Heterodyne Differential Detection

In CPFSK transmission, the signal at each time interval is equal to

$$s(t) = A \cos [\omega_{IF}t \pm \pi \Delta f t + \phi_0] \quad (3.104)$$

where ϕ_0 depends the phase of previous symbol to ensure continuous phase operation and Δf is the frequency deviation between “-1” or “+1”. With a received signal of $r(t) = s(t) + n(t)$, we may define $\tilde{r}(t) = Ae^{\pm j\pi \Delta f t + j\phi_0} + \tilde{n}(t) = A_1(t)e^{j\phi_1(t)}$. The CPFSK signal can be demodulated using the asynchronous receiver of Fig. 3.9 based on the delay-and-multiplier circuit similar to that of Fig. 1.4(b) for DPSK signals. In the CPFSK receiver of Fig. 3.9, the delay is τ instead of the one-bit delay of DPSK signal of T of Fig. 1.4(b). Similar to the case of DPSK signal of Eq. (3.101), the decision random variable is

$$\begin{aligned} r_d &= \tilde{A}_1(t)\tilde{A}_1(t-\tau) \cos [\omega_{IF}\tau + \tilde{\phi}_1(t) - \tilde{\phi}_1(t-\tau)] \\ &= \Re \left\{ \tilde{r}(t)\tilde{r}^*(t-\tau)e^{j\omega_{IF}\tau} \right\}. \end{aligned} \quad (3.105)$$

where $\tilde{\phi}_1(t) = \pm \pi \Delta f t + \phi_0 + \phi_n(t)$ with $\phi_n(t)$ as the phase from $n(t)$. The differential phase is $\tilde{\phi}_1(t) - \tilde{\phi}_1(t-\tau) = \pm \pi \Delta f \tau + \phi_n(t) - \phi_n(t-\tau)$. The optimal system can be designed such that $\omega_{IF}\tau = 2k\pi + \frac{1}{2}\pi$. Without noise, $r_d(t) = \pm A^2 \sin(\Delta f \pi \tau)$. For the best system efficiency, $r_d(t) = \pm A^2$ if $\Delta f \tau = \frac{1}{2}$.

When $\Delta f \tau = \frac{1}{2}$, assume that the phase of noise of $\phi_n(t)$ and $\phi_n(t-\tau)$ are independent of each other, the performance of CPFSK system with differential detection is the same as DPSK system with error probability of

$$p_e = \frac{1}{2} \exp(-\rho_s). \quad (3.106)$$

The most interesting case is $\Delta f = \frac{1}{2T}$ when $\tau = T$ that is the minimum frequency separation for two orthogonal frequencies of Eq. (3.80). The case of $\Delta f = \frac{1}{2T}$ is called minimum shift keying (MSK) modulation. Similar to DPSK signal, MSK may be demodulated based on a one-bit delay and multiplier. The performance of MSK is also the same as DPSK. MSK has a more compact spectrum as compared with DPSK signal.

3.3.5 Heterodyne FSK Discriminator Detection

FSK signal can also be detected by frequency discriminator of Fig. 3.10. The frequency discriminator may be the most popular for analog frequency modulation (FM) system. Frequency discriminator must be operated for system having high SNR.

The two discriminator of Fig. 3.10 are BPF having a frequency response of

$$H_1(f) = \begin{cases} 2\pi K(f - f_{IF}) & f_{IF} < f < f + \Delta f \\ 0 & \text{otherwise} \end{cases} \quad (3.107)$$

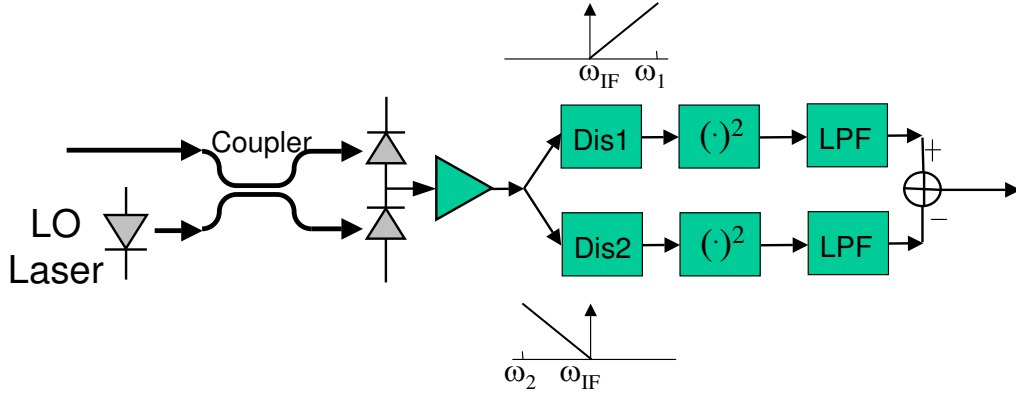


Figure 3.10: A heterodyne asynchronous receiver for FSK signal using frequency discriminator.

and

$$H_2(f) = \begin{cases} 2\pi K(f_{IF} - f) & f - \Delta f < f < f_{IF} \\ 0 & \text{otherwise} \end{cases} \quad (3.108)$$

where K is the slope of the frequency discriminator and Δf is the bandwidth of the frequency discriminator. In time domain, the operation of the frequency discriminator is equivalent to $K \frac{d}{dt}$.

Assume that $s_1(t)$ is transmitted with

$$r(t) = A \cos \omega_1 t + n_1(t) \cos \omega_{IF} t - n_2(t) \sin \omega_{IF} t. \quad (3.109)$$

The output of $H_1(f)$ is

$$\begin{aligned} r_1(t) &= AK(\omega_1 - \omega_{IF}) \sin \omega_1 t \\ &+ K \frac{dn_{11}(t)}{dt} \cos(\omega_{IF} t + \pi \Delta f t) - K \frac{dn_{12}(t)}{dt} \sin(\omega_{IF} t + \pi \Delta f t). \end{aligned} \quad (3.110)$$

where $n_{11}(t)$ and $n_{12}(t)$ are the part of $n_1(t)$ and $n_2(t)$ in the frequency larger than the IF of f_{IF} . The output of $H_2(f)$ is

$$r_2(t) = K \frac{dn_{21}(t)}{dt} \cos(\omega_{IF} t + \pi \Delta f t) - K \frac{dn_{22}(t)}{dt} \sin(\omega_{IF} t + \pi \Delta f t). \quad (3.111)$$

where $n_{21}(t)$ and $n_{22}(t)$ are the part of $n_1(t)$ in the frequency smaller than the IF of f_{IF} . The signal of $r_1(t)$ is similar to an amplitude-modulated signal with a power of $\frac{\pi^2}{2} [AK\Delta f]^2$. The noise of $K \frac{dn_{11}(t)}{dt}$ has an variance of

$$K^2 E \left\{ \left| \frac{dn_{11}}{dt} \right|^2 \right\} = (2\pi K)^2 \int_0^{B_d} N_n f^2 df = (2\pi K)^2 \frac{1}{3} B_d^3 N_n = \frac{4}{3} \pi^2 K^2 B_d^3 \sigma_n^2. \quad (3.112)$$

where N_n is the spectral density of $n_{11}(t)$ and $\sigma_n^2 = N_0 B_d$. The equivalent SNR of the amplitude modulated signal is

$$\rho_{eq} = \frac{\rho_s}{4} \left(\frac{\Delta f}{B_d} \right)^2. \quad (3.113)$$

Similar to the error probability of Eq. (3.97), we obtain

$$p_e = \frac{1}{2} \exp \left[-\frac{3\rho_s}{8} \left(\frac{\Delta f}{B_d} \right)^2 \right]. \quad (3.114)$$

For the case that $\Delta f = B_d$, we obtain $p_e = \frac{1}{2} e^{-3\rho_s/8}$. Using the method basic on frequency discriminator, the system performance is improved with $\Delta f/B_d$. Similar to analog FM, detection based on frequency discriminator expands the signal bandwidth to obtain better system performance. However, the error probability of Eq. (3.114) should consider as an approximation. While the noise outside B_d in Eq. (3.112) does not degrade the system performance, the out of signal band noise provides noise-to-noise beating thought the squarer of Fig. 3.10.

3.3.6 Dual-Filter Detection of Correlated Binary Signals

FSK, DPSK, and MSK are special cases of communications based on two orthogonal signals. The dual-filter detection of FSK signal and differential detection of both DPSK and MSK signals are asynchronous or non-coherent detection of two orthogonal signals. For envelope detection of binary signals, the receiver is the same as that of Fig. 3.8 with the BPF representing two matched filters. If the two signals are correlated with a correlated coefficient of $|\rho|$, the p.d.f. of the outputs of two matched filters are

$$p_1(r_1) = \frac{r_1}{\sigma_n^2} I_0 \left(\frac{r_1 A}{\sigma_n^2} \right) \exp \left(-\frac{r_1^2 + A^2}{2\sigma_n^2} \right), \quad (3.115)$$

$$p_2(r_2) = \frac{r_2}{\sigma_n^2} I_0 \left(\frac{r_2 |\rho| A}{\sigma_n^2} \right) \exp \left(-\frac{r_2^2 + |\rho|^2 A^2}{2\sigma_n^2} \right). \quad (3.116)$$

However, the random variables of R_1 and R_2 are correlated with each other. In order to derive the error probability of $p_e = \Pr\{R_2 > R_1\}$, a transform is required such that $R_2^2 - R_1^2 = \Gamma_2^2 - \Gamma_1^2$ in which the random variables of Γ_2 and Γ_1 are independent of each other and also have Rice distribution. While the amplitude parameter of R_1 and R_2 are A and $|\rho|A$, respectively, the amplitude parameter of Γ_1 and Γ_2 are $A \left[1 \pm \sqrt{1 - |\rho|^2} \right]^{1/2}$, respectively. From Appendix 3.8, the error probability of correlated binary signal with envelope detection is

$$p_e = Q(a, b) - \frac{1}{2} e^{-(a^2+b^2)/2} I_0(ab). \quad (3.117)$$

where

$$\begin{aligned} a &= \sqrt{\frac{\rho_s}{2} \left(1 - \sqrt{1 - |\rho|^2} \right)}, \\ b &= \sqrt{\frac{\rho_s}{2} \left(1 + \sqrt{1 - |\rho|^2} \right)}. \end{aligned} \quad (3.118)$$

For orthogonal signal, $|\rho| = 0$ and $a = 0$ and $b = \sqrt{\rho_s}$, $p_e = Q(0, b) - \frac{1}{2} e^{-b^2/2} = \frac{1}{2} e^{-b^2/2} = \frac{1}{2} e^{-\rho_s/2}$, the same as the error probability of Eq. (3.83).

The error probability of Eq. (3.117) was first derived by Helstrom (1955) based on direct integration. The method to find the error probability here is based on Stein (1964). Proakis (2000) also derives the error probability of Eq. (3.117). While the error probability of Eq. (3.117) is not useful if the two binary signals are well-designed without correlation, degradation that induces correlation can be analyzed based on Eq. (3.117).

3.4 Performance of Direct-Detection Receiver

Other than the IM/DD schemes of Fig. 1.1. Both DPSK and FSK signals can be directly detected without mixing with a LO laser. DPSK and FSK signal can be detected using an interferometer and optical filter, respectively. Direct-detection receiver is simpler than both homodyne or heterodyne receivers that requires a LO laser. This section analyzes the performance of typical direct-detection receiver for ASK or on-off keying signal, DPSK, and FSK signal.

3.4.1 Intensity Modulation Direction-Detection Receiver

Intensity modulation and direction-detection is the simplest optical communication schemes shown in Fig. 1.1. The receiver is just a photodiode that converts the optical intensity into photocurrent. For system limited by amplifier noises, the performance is analyzed in, for example, Agrawal (2002), Becker et al. (1999), Desurvire (1994).

Quantum Limit for Systems Without Amplifier

In a system without amplifier, due to quantum nature of photons, for a mean number of photons of N_s per bit in a binary on-off keying system, the number of photons has a Poisson distribution. The probability of having k photons is

$$p_k = \frac{N_s^k}{k!} e^{-N_s}. \quad (3.119)$$

If the detection is based on the presence or absence of photons, the error probability is

$$p_e = \frac{1}{2} p_0 = \frac{1}{2} e^{-N_s}. \quad (3.120)$$

where the factor of $\frac{1}{2}$ is the probability of “on” state. There is no error for the “off” state with no photon to send. The average number of photons is $\frac{1}{2} N_s$. In order to achieve an error probability or 10^{-9} , an average of 10 photons per bit are required. If the quantum efficiency of η is less than unity, the required number of photons increases by a factor of η^{-1} .

Practical receiver requires thousands number of photons per bit, mostly due to the contribution from thermal noise. As an example, assume a thermal noise density of $i_{th} = 5 \text{ pA}/\sqrt{\text{Hz}}$, corresponding to a receiver sensitivity of -25.2 and -28.2 dBm for 10- and 2.5-Gb/s systems, respectively, if shot noise is ignored and $R = 1$ is assumed. For system operating in $1.55\mu\text{m}$, the number of photons per bit are 4.7×10^4 and 2.3×10^4 for 10- and 2.5-Gb/s systems. Without the usage of optical amplification, practical receiver always require number of photons per bit many order larger than the quantum limit of 9 photons/bit.

Amplifier Noise Limited System

If the system is limited by amplifier noise, the received electric field is

$$E_r(r) = [A_s(t) + n_x(t)]e^{j\omega_c t} \mathbf{x} + n_y(t)e^{j\omega_c t} \mathbf{y}. \quad (3.121)$$

The signal is carried using $A_s(t)$ based on on-off keying. In the direct-detection system, the above electric field converts to photocurrent directly using a photodiode.

$$i(t) = R|A_s(t) + n_x(t)|^2 + R|n_y(t)|^2, \quad (3.122)$$

where shot noise is ignored. If the noise from orthogonal polarization of $n_y(t)$ is ignored, the system is the same as that using envelope detection for heterodyne ASK receiver in Section 3.3.1.

If the common factor of R for the responsivity of photodiode is ignored in Eq. (3.122) for simplicity, assumed an optical matched filter preceding the photodiode, in the on state with $A_s(t) = A$, we obtain

$$r_{\text{on}}(t) = [A + n_{x1}(t)]^2 + n_{x2}^2(t) + n_{y1}^2(t) + n_{y2}^2(t) \quad (3.123)$$

with p.d.f. of

$$p_1(y) = \frac{1}{2\sigma_n^2} \sqrt{\frac{y}{A^2}} e^{-(A^2+y)/2\sigma_n^2} I_1\left(\sqrt{y} \frac{A}{\sigma_n^2}\right), \quad y \geq 0 \quad (3.124)$$

as the noncentral chi-square χ^2 p.d.f. with 4 degrees of freedom.

In the off state with $A_s(t) = 0$, we obtain

$$r_{\text{off}}(t) = n_{x1}^2(t) + n_{x2}^2(t) + n_{y1}^2(t) + n_{y2}^2(t) \quad (3.125)$$

with p.d.f. of

$$p_2(y) = \frac{1}{4\sigma_n^4} y e^{-y/2\sigma_n^2}, \quad y \geq 0 \quad (3.126)$$

With a threshold of y_{th} , the error probability of the system is

$$\begin{aligned} p_e &= \frac{1}{2} \int_0^{y_{\text{th}}} p_1(y) dy + \frac{1}{2} \int_{y_{\text{th}}}^{\infty} p_2(y) dy \\ &= \frac{1}{2} \left[1 - Q_2\left(\frac{A}{\sigma_n}, \frac{\sqrt{y_{\text{th}}}}{\sigma_n}\right) \right] + \frac{1}{2} \exp\left(-\frac{y_{\text{th}}}{2\sigma_n^2}\right) \left(1 + \frac{y_{\text{th}}}{2\sigma_n^2}\right). \end{aligned} \quad (3.127)$$

where

$$Q_2(a, b) = Q(a, b) + e^{-(a^2+b^2)/2} \frac{b}{a} I_1(ab) \quad (3.128)$$

is the second-order generalized Marcum Q function.

The optimal threshold can be determined by

$$\sqrt{y_{\text{th}}} \frac{A}{2\sigma_n^2} = e^{-A^2/2\sigma_n^2} I_1\left(\sqrt{y_{\text{th}}} \frac{A}{\sigma_n^2}\right), \quad y \geq 0. \quad (3.129)$$

In a simplified analysis, we can approximate that $y_{\text{th}} = \frac{1}{4}A^2$, the error probability is approximately equal to

$$p_e \approx \frac{1}{2} \int_{y_{\text{th}}}^{\infty} p_2(y) dy \quad (3.130)$$

$$= \frac{1}{2} \exp\left(-\frac{A^2}{8\sigma_n^2}\right) \left(1 + \frac{A^2}{8\sigma_n^2}\right) \quad (3.131)$$

$$= \frac{1}{2} \exp\left(-\frac{\rho_s}{2}\right) \left(1 + \frac{\rho_s}{2}\right) \quad (3.132)$$

With the inclusion of the amplified noise from orthogonal direction of $n_y(t)$, the error probability is increased by a factor of $1 + \frac{\rho_s}{2}$. Using a direct-detection receiver, based on the error probability of Eq. (3.132), a SNR of $\rho_s = 46.4$ (16.7 dB) is required to achieve an error probability of 10^{-9} . The quantum-limited receiver requires 46.6 photons/bit.

Error Probability Based on Gaussian Approximation

The error probability can be analyzed based on Gaussian approximation with the assumption of two received signals

$$r_{\text{on}}(t) = A + n_1(t), \quad (3.133)$$

$$r_{\text{off}}(t) = n_0(t), \quad (3.134)$$

where $n_0(t)$ and $n_1(t)$ are assumed zero-mean Gaussian noise with variances of $E\{n_1^2(t)\} = \sigma_1^2$ and $E\{n_0^2(t)\} = \sigma_0^2$, respectively. The p.d.f. of the on and off state is

$$p_1(x) = \frac{1}{\sqrt{2\pi}\sigma_1} e^{-(x-A)^2/2\sigma_1^2} \quad (3.135)$$

$$p_0(x) = \frac{1}{\sqrt{2\pi}\sigma_0} e^{-x^2/2\sigma_0^2} \quad (3.136)$$

$$(3.137)$$

The optimal decision threshold can be determined by

$$p_1(x_{\text{th}}) = p_0(x_{\text{th}}), \quad 0 < x_{\text{th}} < A \quad (3.138)$$

of

$$x_{\text{th}} = \frac{\sigma_0 A}{\sigma_0 + \sigma_1}. \quad (3.139)$$

In the derivation of the optimal threshold, we assume that $\sigma_0 \neq \sigma_1$ but $\log(\sigma_1/\sigma_0) = 0$ as an approximation. Without the approximation of $\log(\sigma_1/\sigma_0) = 0$, the optimal threshold is a very complicated formula.

Defined a Q -factor of

$$Q = \frac{A - x_{\text{th}}}{\sigma_1} = \frac{x_{\text{th}}}{\sigma_0} = \frac{A}{\sigma_1 + \sigma_0} \quad (3.140)$$

The error probability is equal to

$$p_e = \frac{1}{2} \text{erfc} \left(\frac{Q}{\sqrt{2}} \right) \quad (3.141)$$

With the Gaussian approximation, the amplitude is equal to

$$A = RP_r \quad (3.142)$$

and the noise variance is equal to

$$\sigma_1^2 = \sigma_{A_s - n_s}^2 + \sigma_{n_s - n_s}^2 + \sigma_{\text{sh}}^2 + \sigma_{\text{th}}^2 \quad (3.143)$$

$$\sigma_0^2 = \sigma_{n_s - n_s}^2 + \sigma_{\text{sh}}^2 + \sigma_{\text{th}}^2 \quad (3.144)$$

where

$$\sigma_{A_s - n_s}^2 = 4R^2 P_r S_{\text{sps}} B_d \quad (3.145)$$

$$\sigma_{n_s - n_s}^2 = 4R^2 S_{\text{sps}}^2 \Delta\nu_{\text{opt}} B_d \quad (3.146)$$

$$\sigma_{\text{sh}}^2 = 2eR(P_r + 2S_{\text{sps}}\Delta\nu_{\text{opt}})B_d \quad (3.147)$$

$$\sigma_{\text{th}}^2 = \frac{4kT}{R_L} \quad (3.148)$$

Thermal noise is included in the above equation for the case that the received signal is very small. A direct-detection on-off keying system is potentially limited by thermal noise instead of amplifier noise.

For the specific cases of Eq. (3.123) and Eq. (3.125), we obtain

$$\sigma_1^2 = 4\sigma_n^2 A^2 + 8\sigma_n^4 \quad (3.149)$$

$$\sigma_0^2 = 8\sigma_n^4 \quad (3.150)$$

and

$$\begin{aligned} Q &= \frac{A^2}{2\sqrt{2}\sigma_n^2 + 2\sigma_n\sqrt{A^2 + 2\sigma_n^2}} \\ &= \frac{\sqrt{2}\rho_s}{1 + \sqrt{2\rho_s + 1}}. \end{aligned} \quad (3.151)$$

Based on the Gaussian approximation, the required SNR to achieve an error probability of 10^{-9} is $\rho_s = 36 + 6\sqrt{2} = 44.5$ (16.5 dB).

When the optical filter preceding the receiver has a wide bandwidth, direct-detection on-off keying system can be approximately analyzed by adding identical and independent noise terms to both Eq. (3.123) and Eq. (3.125) (Humblet and Azizoğlu, 1991, Marcuse, 1990, 1991). The number of noise terms is equal twice the ratio of the optical bandwidth to data rates, the factor of two taking into account the two polarizations of amplifier noises. While Marcuse (1990, 1991) and Humblet and Azizoğlu (1991) sum independent and identical random variables to model amplifier noise, Lee and Shim (1994) sums independent random variables with variance depending on filter response to model amplifier noise. These two methods are also widely used for performance evaluation in direct-detection on-off keying systems (Bosco et al., 2001, Chan and Conradi, 1997, Forestieri, 2000, Holzlohner et al., 2002, Roudas et al., 2002).

Comparison of Different Models

Figure 3.11 shows the error probability of ASK signal detected using various different scheme. The error probability of Eq. (3.67) with synchronous has the lowest error probability for the same SNR ρ_s . The error probability of Eq. (3.91) for envelope detection is also shown for comparison together as the error probability calculated with the optimal threshold of Eq. (3.90) as dashed-lines. The error probability of Eq. (3.132) for direct-detection is shown as solid line with the corresponding error probability calculated with the optimal threshold of Eq. (3.129) as dashed-lines. The error probability with optimal threshold of Eq. (3.129) almost overlaps with Eq. (3.91). The Gaussian approximation of Eq. (3.141) is shown in Fig. 3.11 as dotted-line.

From Fig. 3.11, the performance of system with envelope detection can be evaluated using Eq. (3.91). Compared with the error probability optimal threshold, the approximaton of Eq. (3.91) is just about 0.1 dB worse at the error probability of 10^{-9} .

For direct-detection receiver, the Gaussian approximation overestimates the error probability and gave a penalty of about 0.45 dB comparing with the one with optimal threshold. Because the Gaussian approximation also use an optimal threshold according to its own model, the performance with Gaussian approximation is actually better than the error probability with sub-optimal threshold of Eq. (3.132) by 0.2 dB. In practical system, for both direct-detection or envelope-detection, the error probability of Eq. (3.91) can be used.

3.4.2 Direct-Detected DPSK Receiver

Figure 3.12 redraws the direct-detection receiver for DPSK signal of Fig. 1.4(c). The DPSK receiver uses a Mach-Zehnder interferometer in which the signal is splitted into two paths and combined with a path

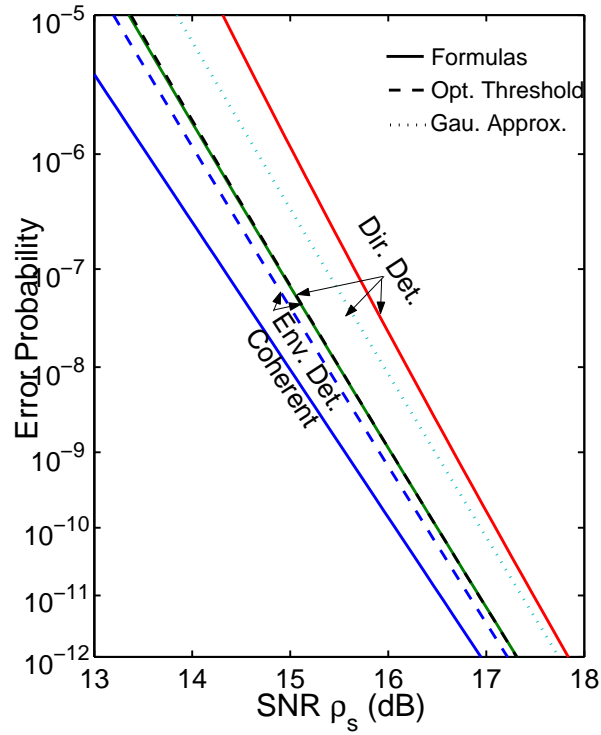


Figure 3.11: The error probability of amplitude-modulated signal as a function of SNR ρ_s .

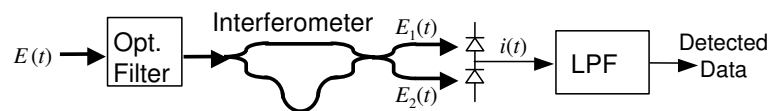


Figure 3.12: Direct detection DPSK receiver using an unpolarized interferometer.

difference of an one-bit delay of T . In practice, the path difference of $\tau \approx T$ must be chosen such that $\exp(j\omega_0\tau) = 1$, where ω_0 is the angular frequency of the signal (Vodhanel, 1989). Ideally, the optical filter before the interferometer is assumed to be a match filter to the transmitted signal. A balanced receiver similar to that of Fig. 3.3 is used to receive the photocurrent. There is a low-pass filter to filter out the receiver noise. We assume that the low-pass filter has a wide bandwidth and does not distort the received signal.

At the output of the unpolarized Mach-Zehnder interferometer, the two optical signals can be expressed as

$$E_1(t) = \frac{\mathbf{x}}{2}[Ae^{-j\phi_s(t)} + n_x(t)] + \frac{\mathbf{y}}{2}n_y(t) + \frac{\mathbf{x}}{2}[Ae^{-j\phi_s(t-T)} + n_x(t-T)] + \frac{\mathbf{y}}{2}n_y(t-T), \quad (3.152)$$

$$E_2(t) = \frac{\mathbf{x}}{2}[Ae^{-j\phi_s(t)} + n_x(t)] + \frac{\mathbf{y}}{2}n_y(t) - \frac{\mathbf{x}}{2}[Ae^{-j\phi_s(t-T)} + n_x(t-T)] - \frac{\mathbf{y}}{2}n_y(t-T). \quad (3.153)$$

In Eq. (3.152) and Eq. (3.153), the path difference of the interferometer is assumed exactly as the symbol time T and $\exp(j\omega_c T) = 1$. The amplifier noises of $n_x(t)$, $n_y(t)$, $n_x(t-T)$, and $n_y(t-T)$ are independent identically distributed complex zero-mean circular Gaussian random variables. The noise variance is $E\{|n_x(t)|^2\} = E\{|n_y(t)|^2\} = E\{|n_x(t-T)|^2\} = E\{|n_y(t-T)|^2\} = 2\sigma_n^2$, where σ_n^2 is the noise variance per dimension. In a polarized receiver, $n_y(t) = n_y(t-T) = 0$ and the error probability is the same as that for heterodyne DPSK system in Sec. 3.3.3.

In Eq. (3.152) and Eq. (3.153), the loss in the interferometer is ignored and the received signal. If the amplifier noise is the dominant noise source, both the interferometer loss and the photodiode responsivity does not affect the system performance.

Without loss of generality, we assume that $\phi_s(t) = \phi_s(t-T) = 0$ when the consecutive transmitted phase are the same. Assume an unity photodiode responsivity, similar to that of Fig. 3.3, the photocurrent at the output of the balanced receiver is

$$i(t) = |E_1(t)|^2 - |E_2(t)|^2, \quad (3.154)$$

where

$$|E_1(t)|^2 = \left| A + \frac{1}{2}[n_x(t) + n_x(t-T)] \right|^2 + \frac{1}{4}|n_y(t) + n_y(t-T)|^2, \quad (3.155)$$

and

$$|E_2(t)|^2 = \frac{1}{4}|n_x(t) - n_x(t-T)|^2 + \frac{1}{4}|n_y(t) - n_y(t-T)|^2. \quad (3.156)$$

The error probability is equal to

$$p_e = \Pr\{i(t) < 0\} = \Pr\{|E_2(t)|^2 > |E_1(t)|^2\}. \quad (3.157)$$

Because $n_x(t) + n_x(t-T)$ is independent of $n_x(t) - n_x(t-T)$ and $n_y(t) + n_y(t-T)$ is independent of $n_y(t) - n_y(t-T)$, $|E_1(t)|^2$ and $|E_2(t)|^2$ are independent of each other. From the error probability of Eq. (3.157), similar to heterodyne DPSK signal in Sec. 3.3.3, DPSK signal can be analyzed as noncoherent detection of an orthogonal binary signal.

The p.d.f. of $|E_1(t)|^2$ of Eq. (3.155) is

$$p_{|E_1|^2}(y) = \frac{1}{2\sigma^2 A} \sqrt{y} \exp\left(-\frac{A^2 + y}{2\sigma^2}\right) I_1\left(\sqrt{y} \frac{A}{\sigma^2}\right), \quad y \geq 0. \quad (3.158)$$

where $I_1(\cdot)$ is the first-order modified Bessel function of the first kind and the variance parameter $\sigma^2 = \frac{1}{2}\sigma_n^2$. The p.d.f. of $p_{|E_1|^2}(y)$ is the noncentral χ -square distribution with four degrees of freedom with a variance parameter of $\sigma^2 = \frac{1}{2}\sigma_n^2$ and noncentrality parameter of A^2 . The variance of $\sigma^2 = \frac{1}{2}\sigma_n^2$ is the variance per dimension of the random variable of $\frac{1}{2}[n_x(t) \pm n_x(t-T)]$ and $\frac{1}{2}[n_y(t) \pm n_y(t-T)]$ in the random variables of Eq. (3.155) and Eq. (3.156).

The p.d.f. of $|E_2(t)|^2$ of Eq. (3.156) is

$$p_{|E_2|^2}(y) = \frac{1}{4\sigma^4} y \exp\left(-\frac{y}{2\sigma^2}\right), \quad y \geq 0. \quad (3.159)$$

The p.d.f. of $p_{|E_2|^2}(y)$ is the χ -square (or Γ) distribution with four degrees of freedom.

First of all, we need to find the probability of (Gradshteyn and Ryzhik, 1980, §3.351)

$$\begin{aligned} \Pr\{|E_2(t)|^2 > y\} &= \int_y^{+\infty} p_{|E_2|^2}(y) dy \\ &= \exp\left(-\frac{y}{2\sigma^2}\right) \left[1 + \frac{y}{2\sigma^2}\right]. \end{aligned} \quad (3.160)$$

The error probability of Eq. (3.157) is

$$p_e = \int_0^{+\infty} \Pr\{|E_2(t)|^2 > y\} p_{|E_1|^2}(y) dy. \quad (3.161)$$

Using the p.d.f. of Eq. (3.158) and the probability of Eq. (3.160), after some simplifications, we get

$$p_e = \frac{e^{-2\rho_s}}{\sqrt{2\rho_s}} \int_0^{+\infty} (1+x)\sqrt{x}e^{-2x} I_1\left(2\sqrt{2\rho_s x}\right) dx, \quad (3.162)$$

where $x = y/(2\sigma^2)$, and $\rho_s = E_0^2/\sigma^2 = E_0^2/(2\sigma_n^2)$ is the SNR. As the special case of (Gradshteyn and Ryzhik, 1980, §6.631), we get $\int_0^\infty x^{1/2}e^{-2x}I_1(a\sqrt{x})dx = (a/8)e^{a^2/8}$ and $\int_0^\infty x^{3/2}e^{-2x}I_1(a\sqrt{x})dx = [a(16+a^2)/128]e^{a^2/8}$. The integration of Eq. (3.162) is

$$p_e = \frac{\exp(-\rho_s)}{2} \left(1 + \frac{\rho_s}{4}\right). \quad (3.163)$$

Comparing the heterodyne error probability in Sec. 3.3.3, with the amplifier noise from the orthogonal polarization, the error probability is increased by a factor of $1 + \rho_s/4$. The increase of the error probability is the same as that for direction-detection ASK signals.

Figure 3.13 shows the error probability of phase-modulated signal as a function of SNR ρ_s . The error probability of synchronous detection of $\frac{1}{2}\text{erfc}\sqrt{\rho_s}$ of Eq. (3.76), the error probability of asynchronous heterodyne differential detection of $\frac{1}{2}e^{-\rho_s}$ of Eq. (3.103), and the error probability of direction-detection of Eq. (3.163) are also shown for comparison. For an error probability of 10^{-9} , asynchronous heterodyne detection is about 0.45 dB worse than synchronous detection, and direct-detection is about 0.40 dB worse than asynchronous differential detection. The quantum-limited receiver requires 18.0, 20.0, and 21.9 photons/bit.

The degradation of direction-detection is due to the inclusion of amplifier noise from orthogonal polarization. If a lossless polarizer precedes the detector, an improvement of 0.4 dB can be expected. In Tonguz and Wagner (1991), direct-detection DPSK receiver performs the same as heterodyne differential detection if the amplifier noise from orthogonal direction is ignored. The error probability of Eq. (3.163) was first derived by Okoshi et al. (1988) for DPSK signals with similar noise characteristics.

If the direct-detection receiver has a noise bandwidth far larger than the signal bandwidth, the system was analyzed in Chinn et al. (1996), Humblet and Azizoglu (1991), Jacobsen (1993). The DPSK error probability of Eq. (3.103) assumes that there are two noise sources of $n_1(t)$ and $n_2(t)$. The error probability of Eq. (3.163) assumes that there are four noise sources of $n_{x1}(t)$, $n_{x2}(t)$, $n_{y1}(t)$, and $n_{y2}(t)$ for both real and imaginary parts noise. With the assumption of both Marcuse (1990) and Humblet and

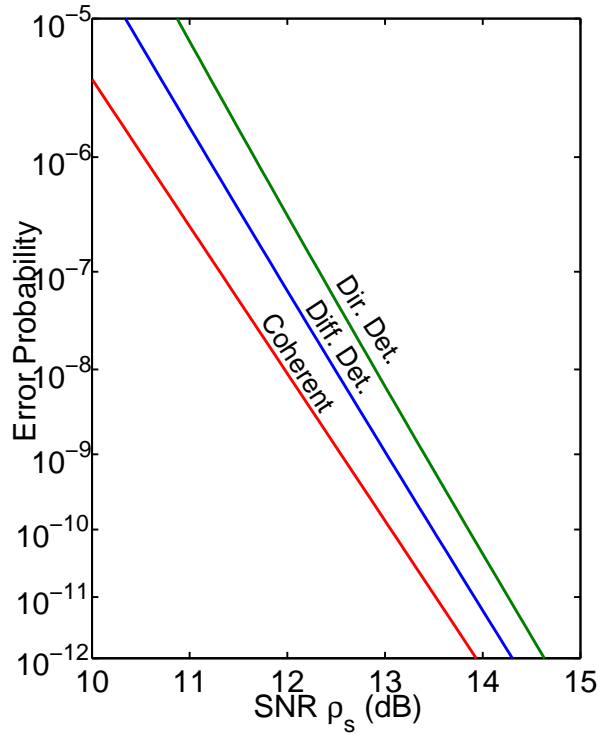


Figure 3.13: The error probability of phase-modulated signal as a function of SNR ρ_s .

Azizoğlu (1991) that there are $2k$ noise sources that are independent of each other, the error probability are

$$p_e = \frac{e^{-\rho_s}}{2} \sum_{m=1}^k h_k \frac{\rho_s^m}{m!} \quad (3.164)$$

where

$$h_k = \frac{1}{2^{2(k-1)}} \sum_{l=0}^{k-1} \binom{2k-l-2}{k-1-l}. \quad (3.165)$$

Direct-detection DPSK signal is unquestionable the most popular coherent optical communication scheme as shown in Table 1.2. DPSK receiver with very good receiver sensitivity was developed by Atia and Bondurant (1999), Gnauck et al. (2003) and Sinsky et al. (2003).

3.4.3 Dual-Filter Direct-Detection of FSK Signal

Figure 3.14 shows a dual-filter direct detection FSK receiver. Figure 3.14(a) is the schematic of the receiver in which a balanced-receiver is used with one detector to the output of each optical filter, respectively. The optical filter can be implemented using fiber Bragg grating or multilayer dielectric filter as shown in Fig. 3.14(b) and (c), respectively. The optical filter centers at the optical frequency of f_1 and f_2 , corresponding to the two frequencies of the FSK signal, respectively.

If the two optical filters are match filter and the two FSK signals are orthogonal with each other, for lossless optical filters,

$$E_1(t) = [A \cos 2\pi f_1 t + n_{x1}(t)] \mathbf{x} + n_{y1}(t) \mathbf{y} \quad (3.166)$$

if $s_1(t)$ with optical frequency of f_1 is transmitted, where n_{x1} and $n_{y1}(t)$ is the amplifier noise in the polarization parallel and orthogonal to the signal, respectively. The noise variance is $E\{|n_{x1}(t)|^2\} =$

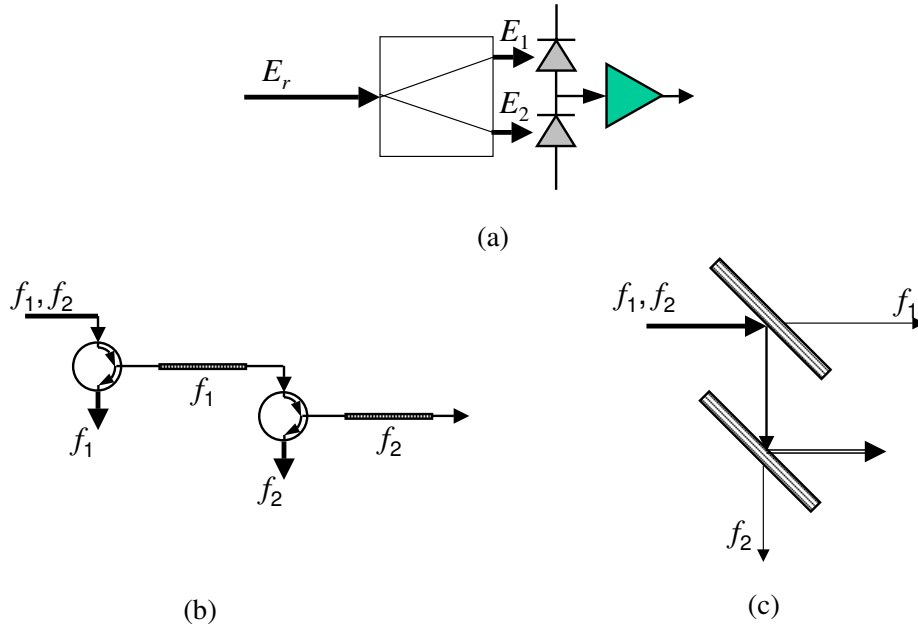


Figure 3.14: Direct detection FSK receiver using two optical filters. (a) The schematic of the receivers. (b) Optical filter using fiber Bragg grating. (c) Optical filter using multilayer dielectric filter

$E\{|n_{y1}(t)|^2\} = \sigma_n^2$ and the SNR is $\rho_s = A^2/2\sigma_n^2$. If $s_1(t)$ is transmitted, the electric field for the optical filter centered at f_2 is

$$E_2(t) = n_{x2}(t)\mathbf{x} + n_{y1}(t)\mathbf{y}. \quad (3.167)$$

With a photocurrent of $i(t) = R|E_1(t)|^2 - R|E_2(t)|^2$ and an error probability of $p_e = \Pr\{i(t) < 0\}$, the error probability is similar to that for DPSK signal of Eq. (3.163). For dual-filter direct-detection FSK receiver, the error probability is

$$p_e = \frac{1}{2} \exp\left(-\frac{\rho_s}{2}\right) \left(1 + \frac{\rho_s}{8}\right). \quad (3.168)$$

Direct-detection FSK signal is 3-dB worse than direct-detection DPSK signal. However, using the same receiver of Fig. 3.12, direct-detection MSK receiver has the same performance as DPSK signal.

Figure 3.15 shows the error probability of FSK signal detected a synchronous receiver, asynchronous heterodyne receiver, and direct-detection dual-filter receiver. Compared with Fig. 3.13, frequency-modulated signal is 3-dB worse than phase-modulated signal. For an error probability of 10^{-9} , asynchronous heterodyne detection is about 0.45 dB worse than synchronous detection, and direct-detection is about 0.40 dB worse than asynchronous differential detection. The quantum-limited receiver requires 36.0, 40.0, and 43.8 photons/bit.

Practical FSK receiver may use a single filter with a performance similar to ASK signal but with 3-dB penalty. If the two optical filters have crosstalk, the outputs of $E_1(t)$ and $E_2(t)$ have correlation and the error probability is similar to Eq. (3.117). In order to improve the performance, FSK signal with large frequency deviation can be used to use bandwidth to obtain better performance. The performance of FSK signal with frequency discriminator is the same as heterodyne system analyzed in Sec. 3.3.2. However, high frequency deviation FSK system has very small spectral efficiency. Direct-detection FSK signal for frequency-modulated signal was used by Olsson and Tang (1979), Saito and Kimura (1964), Saito et al. (1983). Single-filter FSK direct-detection can use Fabry-Perot filter (Chraplyvy et al., 1989, Kaminow, 1990, Kaminow et al., 1988, Malyon, 1990, Willner et al., 1990, Willner, 1990) or ring resonator (Oda et al., 1994, 1991). Using the interferometer of Fig. 3.12, CPFSK signal was directly detected by

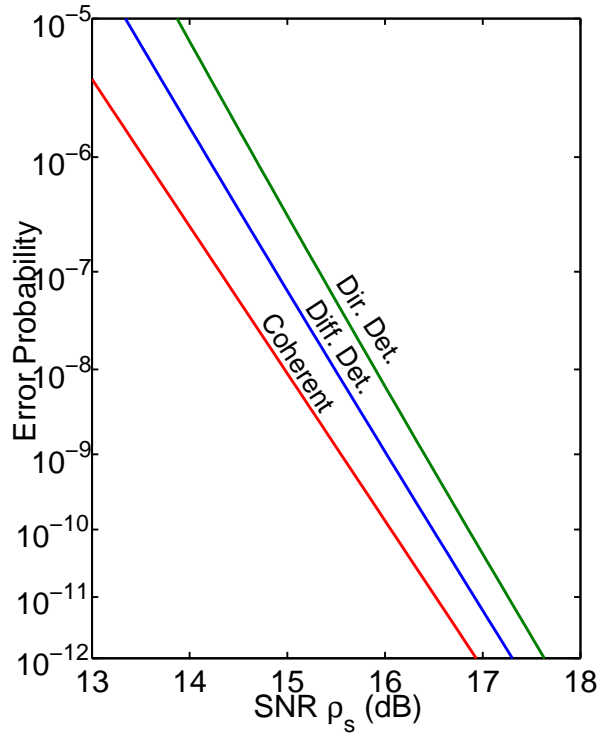


Figure 3.15: The error probability of frequency-modulated signal as a function of SNR ρ_s .

Malyon and Stallard (1989), Toba et al. (1990, 1991). When an optical filter is used to demodulate the FSK signal, it can also function as a demultiplexer to select the WDM channel.

3.5 Phase-Diversity Receiver

Phase-diversity receiver is another type of asynchronous detection for homodyne systems. The phase-diversity receiver is based on the quadrature receiver of Fig. 3.4. From the photocurrent of Eq. (3.48) and Eq. (3.49), including a random phase from either the received signal or the LO signal of θ_0 , we get

$$\begin{aligned} r_I(t) &= A(t) \cos[\phi_s(t) + \theta_0] + n_I(t) \\ r_Q(t) &= A(t) \sin[\phi_s(t) + \theta_0] + n_Q(t) \end{aligned} \quad (3.169)$$

where $A(t)$ is due to amplitude modulation, $\phi_s(t)$ from phase modulation, and $n_I(t)$ and $n_Q(t)$ are the additive Gaussian noise.

3.5.1 Phase-Diversity ASK Receiver

If the signal is amplitude-modulated with $\phi_s(t) = 0$ in the signals of Eq. (3.169), amplitude modulated signal with $A(t) = \{A, 0\}$ is demodulated by

$$r_d(t) = \sqrt{r_I^2(t) + r_Q^2(t)} \quad (3.170)$$

Note that the phase-diversity ASK receiver is similar to heterodyne detector of Section 3.3.1 for envelope detection of heterodyne ASK receiver. The error probability of phase-diversity ASK receiver is the same as Eq. (3.91):

$$p_e = \frac{1}{2} \exp\left(-\frac{\rho_s}{2}\right) \quad (3.171)$$

if is chosen as the $A/2$. As a homodyne phase-diversity ASK receiver is the same as a heterodyne ASK receiver based on envelope detection, other aspects of a homodyne phase-diversity ASK receiver can also be analyzed the same the corresponding receiver in Sec. 3.3.1.

3.5.2 Phase-Diversity DPSK Receiver

If the data in encode in the phase difference of $\phi_s(t) - \phi_s(t - T)$ using DPSK modulation, the amplitude of $A(t) = A$ as a constant. The phase difference can be demodulated using

$$\begin{aligned} r_d(t) &= r_I(t)r_I(t - T) + r_Q(t)r_Q(t - T) \\ &= A^2 \cos[\phi_s(t) - \phi_s(t - T)] + \text{noise terms} \end{aligned} \quad (3.172)$$

Without noise, $r_d(t)$ is proportional to $\cos[\phi_s(t) - \phi_s(t - T)]$ and $r_d(t) = \pm A^2$ when $\phi_s(t) - \phi_s(t - T) = 0$ or π , respectively.

The phase-diversity receiver for DPSK signal has the same performance as a DPSK heterodyne receiver using differential detection of Sec. 3.3.3 or Fig. 3.13 with an error probability of

$$p_e = \frac{1}{2} \exp(-\rho_s). \quad (3.173)$$

3.5.3 Phase-Diversity Frequency Modulated Receiver

For FSK signal, the received signals of Eq. (3.169) at the output of the quadrature homodyne receiver of Fig. 3.4 are

$$\begin{aligned} r_I(t) &= A \cos(\pm\pi\Delta ft) + n_I(t) \\ r_Q(t) &= A \sin(\pm\pi\Delta ft) + n_Q(t) \end{aligned} \quad (3.174)$$

where $\Delta f = (\omega_1 - \omega_2)/(2\pi)$ is the frequency difference between the two FSK signals. The demodulated signal is

$$\begin{aligned} r_d(t) &= r_I(t)\frac{dr_Q(t)}{dt} + r_Q(t)\frac{dr_I(t)}{dt} \\ &= \mp\pi\Delta f A^2 + \text{noise terms.} \end{aligned} \quad (3.175)$$

For FSK signal, the receiver sensitivity increases with the frequency difference of Δf . The performance of the system is similar to that of Sec. 3.3.5.

For CPFSK signal, the output from the receiver is the same as Eq. (3.174) but with continuous phase relationship of

$$\begin{aligned} r_I(t) &= A \cos(\pm\pi\Delta ft + \theta_0) + n_I(t) \\ r_Q(t) &= A \sin(\pm\pi\Delta ft + \theta_0) + n_Q(t) \end{aligned} \quad (3.176)$$

The demodulated signal is

$$\begin{aligned} r_d(t) &= r_I(t)r_Q(t - \tau) + r_Q(t)r_I(t - \tau) \\ &= \pm A^2 \sin(\pi\Delta f\tau) + \text{noise terms.} \end{aligned} \quad (3.177)$$

For MSK signal, $\tau = T$ and $\Delta f = \frac{1}{2T}$, the receiver sensitivity is the same as differential detection DPSK signals of Eq. (3.103) or Fig. 3.13.

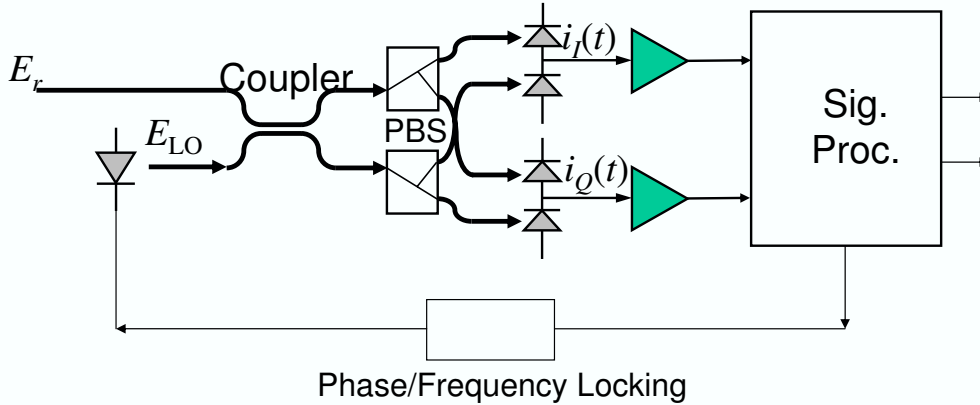


Figure 3.16: A polarization diversity receiver.

Homodyne phase diversity receiver was mostly for ASK and DPSK signals (Cheng et al., 1989, Davis et al., 1987, Davis and Wright, 1986, Hodgkinson et al., 1985, 1988, Kazvosky et al., 1987, Okoshi and Cheng, 1987, Smith, 1987). Phase diversity receiver for FSK and CPFSK modulation is not as popular (Davis et al., 1987, Noe et al., 1988b, Siuzdak and van Etten, 1991, Tsao et al., 1992, 1990). Reviewed by Kazovsky (1989), phase diversity receiver was also analyzed by Hao and Wicker (1995), Ho and Wang (1995), Nicholson and Stephens (1989), Siuzdak and van Etten (1989), especially those using 120° optical hybrid. The primary advantage of phase-diversity is the usage of homodyne detection to save the required bandwidth.

In term of performance for system limited by optical amplifier noise, phase-diversity receiver performs about 0.4 dB better than direct-detection receiver for an error probability of 10^{-9} . The main advantage of phase diversity receiver is to provide close channel spacing or reduce the bandwidth requirement of the receiver. Compared with the image-rejection heterodyne receiver of Sec. 3.1.4, the advantage of phase diversity receiver is the same as that of image-rejection heterodyne receiver. Both phase-diversity homodyne or image-rejection heterodyne receiver use the same optical front-end of Fig. 3.4 with a 90° optical hybrid.

3.6 Polarization Diversity Receiver

The single branch receiver of Fig. 3.1 and the balanced receiver of Fig. 3.3 all requires polarization control to match the polarization of received signal with that of the LO laser. The image-rejection receiver of Fig. 3.5 requires polarization control such that the polarization of the received signal is linear polarized to 45° with respect to the polarizer. System without polarization control is possible using polarization diversity techniques.

Figure 3.16 shows a polarization diversity receiver with an optical front end similar to a 90° optical hybrid of Fig. 3.4. However, unlike the 90° optical hybrid with linearly polarized received signal, the received optical field of the polarization diversity receiver is generally elliptically polarized. The LO laser is linearly polarized at 45° with respect to the receiver polarizer. The received signal is mixed with the LO using a 3-dB coupler and feeds to two separated polarization beam splitter.

Assuming that the received signal has an electric field

$$E_r(t) = A_s(t) \left[\cos \varphi \mathbf{x} + \sin \varphi e^{i\theta} \mathbf{y} \right] e^{j\omega_c t + j\phi_s(t)} \quad (3.178)$$

where the angles of φ and θ are relative to received polarizer. The LO laser has an electric field of

$$E_{LO}(t) = \frac{A_L}{\sqrt{2}} (\mathbf{x} + \mathbf{y}) e^{j\omega_{LO} t}. \quad (3.179)$$

The electric fields at the outputs of the 3-dB coupler are

$$\begin{aligned}
E_1(t) &= \frac{1}{\sqrt{2}} [E_r(t) + E_{LO}(t)] \\
&= \frac{\mathbf{x}}{2} \left[A_s(t) \cos \varphi e^{j\omega_c t + j\phi_s(t)} + A_L e^{j\omega_{LO} t} \right] \\
&\quad + \frac{\mathbf{y}}{2} \left[A_s(t) \sin \varphi e^{j\omega_c t + j\phi_s(t) + j\theta} + A_L e^{j\omega_{LO} t} \right], \tag{3.180}
\end{aligned}$$

and

$$\begin{aligned}
E_2(t) &= \frac{1}{\sqrt{2}} [E_r(t) - E_{LO}(t)] \\
&= \frac{\mathbf{x}}{2} \left[A_s(t) \cos \varphi e^{j\omega_c t + j\phi_s(t)} - A_L e^{j\omega_{LO} t} \right] \\
&\quad + \frac{\mathbf{y}}{2} \left[A_s(t) \sin \varphi e^{j\omega_c t + j\phi_s(t) + j\theta} - A_L e^{j\omega_{LO} t} \right]. \tag{3.181}
\end{aligned}$$

The photocurrents at the output of the two balanced receivers are

$$i_I(t) = \cos \varphi R A_s(t) A_L \cos[\omega_{IF} t + \phi_s(t)] \tag{3.182}$$

and

$$i_Q(t) = \sin \varphi R A_s(t) A_L \cos[\omega_{IF} t + \phi_s(t) + \theta]. \tag{3.183}$$

In the both photocurrents of Eq. (3.182) and Eq. (3.183), the additive noise has the same variance and independent of each other. With noise, the received signal is $i_I(t) + n_I(t)$ and $i_Q(t) + n_Q(t)$ where $E\{n_I^2(t)\} = E\{n_Q^2(t)\} = \sigma_n^2$.

3.6.1 Combination of Polarization Diversity

The polarization diversity scheme is applicable to various modulation schemes. Data are demodulated by combining the information from two branches. The photocurrents can be processed in either the IF or the baseband. If the signal are combined in the IF stage, the carrier phase must be matched to cancel the phase mismatch due to θ in Eq. (3.183). The phase difference of θ changes due to external disturbance, it is necessary to adjust the phases of two signals adaptively before the combination process. In baseband combination, the signal of either $A_s(t)$ or $\phi_s(t)$ are demodulated independently for each polarization component. If the demodulation process track out the phase fluctuation of the IF signals, phase matching is not necessary. In practice, baseband combining is more practical. Here, we assume that the signal after processing is

$$r_i(t) = \cos \varphi A_s(t) \cos \phi_s(t) + n_i(t) \tag{3.184}$$

and

$$r_q(t) = \sin \varphi A_s(t) \cos \phi_s(t) + n_q(t), \tag{3.185}$$

corresponding to the in- and quadrature-phase components.

In each of the method to combine the two polarization components, the optimal weighting is maximum ratio. The in-phase components of Eq. (3.182) is given a gain of $\cos \varphi$ and the quadrature-phase components of Eq. (3.183) is given a gain of $\sin \varphi$. With maximum ratio combination, the combined signal is

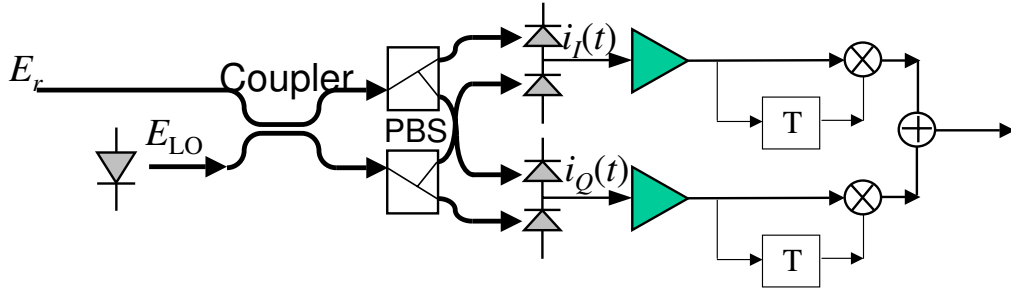


Figure 3.17: A polarization diversity receiver for DPSK or MSK signals.

$$\begin{aligned}
 r_c(t) &= \cos \varphi r_i(t) + \sin \varphi r_q(t) \\
 &= A_s(t) \cos \phi_s(t) + \cos \varphi n_i(t) + \sin \varphi n_q(t)
 \end{aligned} \tag{3.186}$$

where the signal is the same as that with polarization control and the noise is also Gaussian noise having the same variance of $n_i(t)$ and $n_q(t)$. With maximum ratio combination, there is no penalty using polarization diversity.

The simplest combining scheme may be equal-gain combining with a combined signal of

$$\begin{aligned}
 r_c(t) &= r_i(t) + r_q(t) \\
 &= (\cos \varphi + \sin \varphi) A_s(t) \cos \phi_s(t) + n_i(t) + n_q(t)
 \end{aligned} \tag{3.187}$$

The penalty due to equal-gain combining is

$$\delta_p = \frac{(\cos \varphi + \sin \varphi)^2}{2} = \frac{1 + \sin(2\varphi)}{2}, \quad 0 < \varphi < \frac{\pi}{2} \tag{3.188}$$

Selection combining scheme select the polarization components with the largest power. The penalty due to selection combining is

$$\delta_p = \max(\cos^2 \varphi, \sin^2 \varphi) = \frac{1}{2} (1 + |\cos(2\varphi)|), \quad 0 < \varphi < \frac{\pi}{2} \tag{3.189}$$

Another combining scheme can be used for either heterodyne or homodyne ASK signal to square and combined the two signal. The combined signal is

$$\begin{aligned}
 r_c(t) &= r_i^2(t) + r_q^2(t) \\
 &= A_s^2(t) \cos^2 \phi_s(t) + 2A_s(t) \cos \phi_s(t) [n_i(t) + n_q(t)] n_i^2(t) + n_q^2(t).
 \end{aligned} \tag{3.190}$$

In homodyne detection, this combining scheme is only possible for ASK signal in which $\phi_s(t) = 0$ and $A_s(t) = \{A, 0\}$. In heterodyne scheme, square combination is possible for both DPSK or FSK signals with envelope detection.

3.6.2 Polarization Diversity Receiving for Differentially Detected Signals

Figure 3.17 show a polarization-diversity receiver for both DPSK and MSK signals using delay-and-multiplier circuits. Without loss generality and assumes a DPSK signal, after the delay-and-multiplier circuit, the upper branch of Fig. 3.17 has a signal of

$$r_1(t) = \cos^2 \varphi A^2 \cos[\phi_s(t) - \phi_s(t - T)] + \text{noise terms}, \quad (3.191)$$

and the lower branch of Fig. 3.17 has a signal of

$$r_2(t) = \sin^2 \varphi A^2 \cos[\phi_s(t) - \phi_s(t - T)] + \text{noise terms}. \quad (3.192)$$

The overall received signal is

$$r_d(t) = A^2 \cos[\phi_s(t) - \phi_s(t - T)] + \text{noise terms}. \quad (3.193)$$

In the above two equations, the common factor of $\frac{1}{2}R^2$ is ignored. If all noise terms are written down, the noise statistics is the same as that of direct-detection DPSK signal in Sec. 3.4.2 with the error probability of Eq. (3.163). The error probability of Eq. (3.163) was first derived by Okoshi et al. (1988) for phase-diversity DPSK signals. MSK signal should also have the same performance. From Fig. 3.13, the degradation of phase-diversity DPSK or MSK signals is about 0.40 dB compared with heterodyne DPSK signal.

When FSK signal is detected through envelope detection of Fig. 3.8 based on two filters, the signal passes through a squarer. For envelope detection of FSK signal, the detection variable is not sensitivity to θ of Eq. (3.183). When the detected signal from two branches of Fig. 3.16 are combined together, the combination is actually based on square combination and has a degradation of 0.40 dB as from Fig. 3.13.

First suggested by Okoshi (1985, 1986) for combination in IF, polarization diversity has been considered mostly for DPSK and FSK signals using baseband combination (Cline et al., 1990, Glance, 1987, Imai et al., 1991, Kavehrad and Glance, 1988, Okoshi and Cheng, 1987, Ryu et al., 1987, 1991, Shibutani and Yamazaki, 1989).

3.7 Polarization Shift Keying Modulation

An optical fiber can support to polarizations and the electric field in an optical fiber can generally be expressed as

$$E_r(t) = [E_x(t)\mathbf{x} + E_y(t)\mathbf{y}] e^{j\omega_c t}. \quad (3.194)$$

The above express of Eq. (3.194) is in principle the same as Eq. (3.178). In the single branch receiver of Fig. 3.1, we assume that the signal of Eq. (3.2) has a single polarization and aligned with the reference polarization of the receiver of \mathbf{x} .

Comparing the electric field of Eq. (3.194) with Eq. (3.1), both $E_x(t)$ and $E_y(t)$ can be used independently to transmit two data streams using polarization-division multiplexing (PDM). In PDM system, a polarization beam splitter followed a polarization controller is used to separate $E_x(t)$ and $E_y(t)$. The two data streams encode in $E_x(t)$ and $E_y(t)$ are then decoded independently.

The electric fields of $E_x(t)$ and $E_y(t)$ of Eq. (3.194) can be used together to enable polarization-shift keying (PolSK). In the simplest PolSK scheme is to transmit

$$s_1(t) = A\mathbf{x}e^{j\omega_c t}, \quad (3.195)$$

and

$$s_2(t) = A\mathbf{y}e^{j\omega_c t} \quad (3.196)$$

with $E_x(t) = E_y(t) = A$ but used alternatively for “0” or “1”. The performance of this very simple PolSK scheme is identical to that of FSK signal with two orthogonal binary signals. Similar to FSK signal, a PolSK signal can be directly demodulated using a polarization beam splitter, followed by a balanced receiver. The error probability of direct-detection PolSK is that of Eq. (3.83) of

$$p_e = \frac{1}{2}e^{-\rho_s/2} \quad (3.197)$$

Table 3.2: Comparison of Different Optical Receiver for Error Probability of 10^{-9}

Modulation Format	Sensitivity (photons/bit)		Penalty (dB)
	Shot-Noise Limited	Amplifier-Noise Limited	
Homodyne PSK	9	18	0
Heterodyne PSK	18	18	0
Heterodyne DPSK, MSK	20	20	0.45
Direct-Detection DPSK	–	22	0.85
Homodyne ASK	18	36	3
Heterodyne ASK, FSK	36	36	3
Envelope Detected Heterodyne ASK	39	39	3.4
Direct-Detection ASK, FSK	–	40	3.5
Dual-Filter FSK, PolSK	40	40	3.5
Single-Filter FSK	80	80	6.5

because each polarization branch filters output the amplifier noise from orthogonal polarizations. When a heterodyne receiver is used, the LO laser can have a polarization that is 45° to both \mathbf{x} and \mathbf{y} . The performance of heterodyne receiver is also the same as that of Eq. (3.83).

Direct-detection polarization modulation has a long history (Daino et al., 1974, Pratt, 1966). For coherent optical communications, PolSK was proposed mainly to overcome laser phase noise (Benedetto and Poggiolino, 1990, Betti et al., 1988, Calvani et al., 1988, Dietrich et al., 1987, Imai et al., 1990). When polarization is described based on the Stokes parameter, Dietrich et al. (1987) used the s_1 parameter, Calvani et al. (1988) detected the s_2 parameter, Imai et al. (1990) based on the differential s_1 parameter, and Betti et al. (1988) and Benedetto and Poggiolino (1990) detects all Stokes parameters without optical polarization control and use electronic circuits to find the correct polarization states of the received signal. While PolSK system is usually based on heterodyne system, homodyne PolSK systems are described in Betti et al. (1991). PolSK systems are analyzed in details by (Benedetto et al., 1995a,b, Benedetto and Poggiolini, 1992).

3.8 Comparison of Optical Receiver

Table 3.2 shows the performance of a quantum-limited optical receiver for various types of signal. An optimal receiver is assumed in Table 3.2 with, for example, optimal threshold setting. The SNR penalty is also calculated in Table 3.2 compared with a homodyne or heterodyne PSK receiver limited by amplifier noise.

Based on the square combination, polarization diversity receiver has the performance the same as direct-detection receiver. If the optimal combination based on maximum ratio is used, polarization diversity receiver has the same performance as either homodyne or heterodyne receiver. Phase diversity receiver has the same performance as envelope detected receiver.

[A]The Marcum Q Function

For a Gaussian random variable of $A + n_1(t)$ and $n_2(t)$, the amplitude of $R = \sqrt{[A + n_1(t)]^2 + n_2^2(t)}$ has a Rice distribution of

$$p(r) = \frac{r}{\sigma_n^2} I_0 \left(\frac{rA}{\sigma_n^2} \right) \exp \left(-\frac{r^2 + A^2}{2\sigma_n^2} \right). \quad (198)$$

The cumulative distribution function of Rice distribution is

$$\int_x^{+\infty} p(r) dr = Q \left(\frac{A}{\sigma_n}, \frac{x}{\sigma_n} \right), \quad (199)$$

where the Marcum Q function was first used for radar theory (Marcum, 1960) and is very useful in noncoherent or asynchronous detection of orthogonal functions. This appendix presented some important properties of Marcum Q functions. The Marcum Q function is a real function of

$$Q(a, b) = \int_b^{\infty} x I_0(ax) \exp \left(-\frac{x^2 + a^2}{2} \right) dx, \quad (200)$$

or

$$Q(\sqrt{2a}, \sqrt{2b}) = \int_b^{\infty} e^{-(a+x)} I_0(2\sqrt{ax}) dx, \quad (201)$$

where $I_0(x)$ is the zeroth-order modified Bessel function of the first kind. From the definition, we have

$$Q(0, b) = e^{-b^2/2}, \quad (202)$$

$$Q(a, 0) = 1. \quad (203)$$

If $I_0(x)$ is represented as inverse Laplace transform of

$$I_0(2\sqrt{ab}) = \frac{1}{2\pi j} \int_{c-j\infty}^{c+j\infty} \frac{1}{p} \exp \left(ap + \frac{b}{p} \right) dp, \quad c > 0 \quad (204)$$

where c is a real positive number. Substitute Eq. (204) into the Marcum Q function of Eq. (200) and exchange the order of integration, we get

$$\begin{aligned} Q(\sqrt{2a}, \sqrt{2b}) &= \frac{e^{-a}}{2\pi j} \int_{c-j\infty}^{c+j\infty} \frac{1}{p} \int_b^{\infty} e^{-x} \exp \left(ap + \frac{x}{p} \right) dx dp \\ &= e^{-(a+b)} \frac{1}{2\pi j} \int_{c-j\infty}^{c+j\infty} \frac{\exp \left(ap + \frac{b}{p} \right)}{p-1} dp, \quad c > 1 \end{aligned} \quad (205)$$

or

$$Q(\sqrt{2a}, \sqrt{2b}) = e^{-(a+b)} \frac{1}{2\pi j} \int_{c-j\infty}^{c+j\infty} \frac{\exp \left(bp + \frac{a}{p} \right)}{p(p-1)} dp, \quad 0 < c < 1 \quad (206)$$

and

$$Q(a, b) = -e^{-(a^2+b^2)/2} \frac{1}{2\pi j} \int_{c-j\infty}^{c+j\infty} \frac{\exp \left(\frac{b^2 p}{2} + \frac{a^2}{2p} \right)}{p(p-1)} dp, \quad 0 < c < 1 \quad (207)$$

When the characteristic function is used to derive the error probability of a communication system, the above formulas are useful.

By straightforward residue calculation involving shifting of the path, one immediately also derives the useful symmetry relationships

$$Q(a, b) + Q(b, a) = 1 + e^{-(a^2+b^2)/2} I_0(ab) \quad (208)$$

$$Q(a, a) = \frac{1}{2} + \frac{1}{2} e^{-a^2} I_0(a^2) \quad (209)$$

The Marcum Q function can be calculated in terms of function series of

$$Q(a, b) = e^{-(a^2+b^2)/2} \sum_{m=0}^{\infty} \left(\frac{a}{b}\right)^m I_m(ab) \quad b > a \quad (210)$$

$$= 1 - e^{-(a^2+b^2)/2} \sum_{m=0}^{\infty} \left(\frac{b}{a}\right)^m I_m(ab) \quad a > b \quad (211)$$

In the derivation of the error probability of orthogonal modulation with correlation, we need to evaluate the probability that a Rice distribution exceeds another. If the envelope of two Gaussian process, R_1 and R_2 , are independently distributed, with the well-known Rice probability density functions of

$$p_{R_1}(r_1) = \frac{r_1}{\sigma_1^2} \exp\left(-\frac{A_1^2 + r_1^2}{2\sigma_1^2}\right) I_0\left(\frac{A_1 r_1}{\sigma_1^2}\right), \quad (212)$$

$$p_{R_2}(r) = \frac{r_2}{\sigma_2^2} \exp\left(-\frac{A_2^2 + r_2^2}{2\sigma_2^2}\right) I_0\left(\frac{A_2 r_2}{\sigma_2^2}\right), \quad (213)$$

The probability of error is simply

$$\begin{aligned} p_e &= \Pr\{R_1^2 < R_2^2\} = \Pr\{R_1 < R_2\} \\ &= \int_0^{\infty} p_{R_1}(r_1) \int_{r_1}^{\infty} p_{R_2}(r_2) dr_2 dr_1 \\ &= \int_0^{\infty} p_{R_1}(r_1) Q\left(\frac{A_2}{\sigma_2}, \frac{r_1}{\sigma_2}\right) dr_1 \end{aligned} \quad (214)$$

By using Eq. (205) in Eq. (214), interchanging orders of integrations, we may derive

$$\begin{aligned} p_e &= \exp\left[-\frac{1}{2}\left(\frac{A_1^2}{\sigma_1^2} + \frac{A_2^2}{\sigma_2^2}\right)\right] \\ &\quad \times \frac{1}{2\pi j} \int_{c-j\infty}^{c+j\infty} \frac{\exp\left(\frac{A_2^2}{2\sigma_2^2} p\right)}{p-1} \frac{1}{1 + \frac{\sigma_1^2}{\sigma_2^2}\left(1 - \frac{1}{p}\right)} \\ &\quad \times \exp\left[\frac{A_1^2}{2\sigma_1^2} \frac{1}{1 + \frac{\sigma_1^2}{\sigma_2^2}\left(1 - \frac{1}{p}\right)}\right] dp \quad c > 1 \end{aligned} \quad (215)$$

Using the obvious partial fraction expansion, after some algebra via Eq. (204) and Eq. (205), the error probability is

$$p_e = Q(a, b) - \frac{\sigma_1^2}{\sigma_1^2 + \sigma_2^2} e^{-(a^2+b^2)/2} I_0(ab) \quad (216)$$

where

$$a^2 = \frac{A_2^2}{\sigma_1^2 + \sigma_2^2}, \quad b^2 = \frac{A_1^2}{\sigma_1^2 + \sigma_2^2}. \quad (217)$$

The results of Eq. (216) can also be written in more symmetric forms of

$$p_e = \frac{\sigma_1^2}{\sigma_1^2 + \sigma_2^2} [1 - Q(b, a)] + \frac{\sigma_2^2}{\sigma_1^2 + \sigma_2^2} Q(a, b), \quad (218)$$

and

$$p_e = \frac{1}{2} [1 - Q(b, a) + Q(a, b)] - \frac{\sigma_1^2 - \sigma_2^2}{\sigma_1^2 + \sigma_2^2} e^{-(a^2+b^2)/2} I_0(ab). \quad (219)$$

Bibliography

- Aarts, W. H. J. and Khoe, G. D. (1989). New endless polarization control method using three fiber squeezers. *J. Lightwave Technol.*, 7(7):1033–1043.
- Abbas, G. L., Chan, V. W. S., and Yee, T. K. (1985). A dual-detector optical heterodyne receiver for local oscillator noise suppression. *J. Lightwave Technol.*, LT-3(5):1110–1122.
- Agrawal, G. P. (2002). *Fiber-Optic Communication Systems*. Wiley-Interscience, New York, 3 edition.
- Atia, W. A. and Bondurant, R. S. (1999). Demonstration of return-to-zero signaling in both OOK and DPSK formats to improve receiver sensitivity in an optically preamplifier receiver. In *Proc. LEOS '99*. paper TuM3.
- Becker, P. C., Olsson, N. A., and Simpson, J. R. (1999). *Erbium-Doped Fiber Amplifiers: Fundamental and Technology*. Academic Press, San Diego.
- Benedetto, S., Gaudino, R., and Poggiolini, P. (1995a). Direct detection of optical digital transmission based on polarization shift keying modulation. *IEEE J. Sel. Areas Commun.*, 13(3):531–542.
- Benedetto, S., Gaudino, R., and Poggiolini, P. (1995b). Performance of coherent optical polarization shift keying modulation in the presence of phase noise. *IEEE Trans. Commun.*, 43:1603–1612.
- Benedetto, S. and Poggiolini, P. (1992). Theory of polarization shift keying modulation. *IEEE Trans. Commun.*, 40(4):708–721.
- Benedetto, S. and Poggiolino, P. (1990). Performance evaluation of polarisation shift keying modulation schemes. *Electron. Lett.*, 26(4):256–258.
- Betti, S., Curti, T., Daino, B., de Marchis, G., and Iannone, E. (1988). State of polarisation and phase noise independent coherent optical transmission system based on Stokes parameter detection. *Electron. Lett.*, 24(23):1460–1461.
- Betti, S., de Marchis, G., and Iannone, E. (1995). *Coherent Optical Communication Systems*. Wiley, New York.
- Betti, S., De Marchis, G., Iannone, E., and Lazzaro, P. (1991). Homodyne optical coherent systems based on polarization modulation. *J. Lightwave Technol.*, 9(10):1314–1320.
- Bosco, G., Carena, A., Curri, V., Gaudino, R., Poggiolini, P., and Benedetto, S. (2001). A novel analytical approach to the evaluation of the impact of fiber parametric gain on the bit error rate. *IEEE Trans. Commun.*, 49(12):2154–2163.
- Cahn, C. R. (1959). Performance of digital phase-modulation communication systems. *IRE Trans. Commun. Sys.*, CS-7(1):3–6.
- Calvani, R., Caponi, R., and Cisternino, F. (1988). Polarization phase-shift keying: A coherent transmission technique with differential heterodyne detection. *Electron. Lett.*, 24(10):642–643.
- Chan, B. and Conradi, J. (1997). On the non-Gaussian noise in Erbium-doped fiber amplifiers. *J. Lightwave Technol.*, 15(4):680–687.
- Cheng, Y. H., Okoshi, T., and Ishida, O. (1989). Performance analysis and experiment of a homodyne receiver insensitive to both polarization and phase fluctuations. *J. Lightwave Technol.*, 7(2):368–374.

- Chikama, T., Naito, T., Watanabe, S., Kiyonaga, T., Suyama, M., and Kuwahara, H. (1990). Optical heterodyne image-rejection receiver for high-density optical frequency division multiplexing system. *J. Lightwave Technol.*, 8(6):1087–1093.
- Chinn, S. R., Boroson, D. M., and Livas, J. C. (1996). Sensitivity of optically preamplified DPSK receivers with Fabry-Perot filters. *J. Lightwave Technol.*, 14(3):370–376.
- Chraplyvy, A. R., Tkach, R. W., Gnauck, A. H., Kasper, B. L., and Derosier, R. (1989). 8 Gbit/s FSK modulation of DFB lasers with optical demodulation. *Electron. Lett.*, 25(5):319–321.
- Cline, T. W., Delavaux, J.-P. M., Dutta, N. K., Eijk, P. V., Kuo, C. Y.; Owen, B., Park, Y. K., Pleiss, T. C., Riggs, R. S., Tench, R. E., Twu, Y., and Tzeng, L. D.; Wagner, E. J. (1990). A field demonstration of 1.7 Gb/s coherent lightwave regenerators. *IEEE Photon. Technol. Lett.*, 2(6):425–427.
- Cvijetic, M. (1996). *Coherent and Nonlinear Lightwave Communications*. Artech House, Boston.
- Daino, B., Galeotti, M., and Sette, D. (1974). Error-rate measurements in an atmospheric twin-channel optical link. *IEEE J. Quantum Electron.*, QE-10(1):86–87.
- Darcie, T. E. and Glance, B. (1986). Optical heterodyne image-rejection mixer. *Electron. Lett.*, 22:825–826.
- Davis, A. W., Pettitt, M. J., King, J. P., and Wright, S. (1987). Phase diversity techniques for coherent optical receivers. *J. Lightwave Technol.*, LT-5(4):561–572.
- Davis, A. W. and Wright, S. (1986). Coherent optical receiver for 680 Mbit/s using phase diversity. *Electron. Lett.*, 22(1):9–11.
- Delavaux, J.-M. P., Park, Y. K., Barski, S., Lefevre, H., Failes, M., and Warner, C. (1990). All-fibre optical hybrid for coherent polarisation diversity receivers. *Electron. Lett.*, 16(16):1303–1305.
- Delavaux, J.-M. P. and Riggs, R. (1990). High performance packaged optical coherent hybrid. *Electron. Lett.*, 16(14):1022–1024.
- Desurvire, E. (1994). *Erbium-Doped Fiber Amplifiers*. John Wiley & Sons, New York.
- Dietrich, E., Enning, B., Gross, B., and Knupke, E. (1987). Heterodyne transmission of a 560 Mbit/s optical signal by means of polarisation shift keying. *Electron. Lett.*, 23:421–422.
- Forestieri, E. (2000). Evaluating the error probability in lightwave systems with chromatic dispersion, arbitrary pulse shape and pre- and postdetection filtering. *J. Lightwave Technol.*, 18(11):1493–1503.
- Glance, B. (1987). Polarization independent coherent optical receiver. *J. Lightwave Technol.*, LT-5(2):274–276.
- Glance, B., Eisenstein, G., Fitzgerald, P. J., Pollock, K. J., and Raybon, G. (1988). Sensitivity of an optical heterodyne receiver in presence of an optical preamplifier. *Electron. Lett.*, 24(19):1229–1230.
- Glance, B. S. (1986). An optical heterodyne mixer providing image-frequency rejection. *J. Lightwave Technol.*, LT-4(11):1722–1725.
- Gnauck, A. H., Chandrasekhar, S., Leuthold, J., and Stulz, L. (2003). Demonstration of 42.7-Gb/s DPSK receiver with 45 photon/bit sensitivity. *IEEE Photon. Technol. Lett.*, 15(1):99–101.
- Goodwin, F. E. (1967). A 3.39-micron infrared optical heterodyne communication system. *IEEE J. Quantum Electron.*, QE-3(11):524–531.
- Gradshteyn, I. S. and Ryzhik, I. M. (1980). *Table of Integrals, Series, and Products*. Academic Press, San Diego.
- Hao, M.-J. and Wicker, S. B. (1995). Performance evaluation of FSK and CPFSK optical communication systems: a stable and accurate method. *J. Lightwave Technol.*, 13(8):1613–1623.
- Helstrom, C. W. (1955). The resolution of signals in white Gaussian noise. *Proc. IRE*, 43(9):1111–1118.
- Ho, C.-L. and Wang, J.-N. (1995). Calculating the performance of optical cpfsk phase diversity receivers. *J. Lightwave Technol.*, 13(5):971–976.

- Hodgkinson, T. G., Harmon, R. A., and Smith, D. W. (1985). Demodulation of optical DPSK using in-phase and quadrature detection. *Electron. Lett.*, 21(21):867–868.
- Hodgkinson, T. G., Harmon, R. A., Smith, D. W., and Chidgey, P. J. (1988). In-phase and quadrature detection using 90° optical hybrid receiver: experiments and design considerations. *IEE Proc. J*, 135(3):260–267.
- Hoffman, D., Heidrich, H., Wenke, G., Langenhorst, R., and Dietrich, E. (1989). Integrated optics eight-port 90° hybrid on LiNbO₃. *J. Lightwave Technol.*, 7(5):794–798.
- Holzlohner, R., Grigoryan, V. S., Menyuk, C. R., and Kath, W. L. (2002). Accurate calculation of eye diagrams and bit error rates in optical transmission systems using linearization. *J. Lightwave Technol.*, 20(3):389–400.
- Hooijmans, P. W. (1994). *Coherent Optical System Design*. John Wiley & Sons, New York.
- Humblet, P. A. and Azizoğlu, M. (1991). On the bit error rate of lightwave systems with optical amplifiers. *J. Lightwave Technol.*, 9(11):1576–1582.
- Imai, T., Ohkawa, N., Hayashi, Y., and Ichihashi, Y. (1991). Polarization diversity detection performance of 2.5-Gb/s CPFSK regenerators intended for field use. *J. Lightwave Technol.*, 9(6):761–769.
- Imai, Y., Iizuka, K., and James, R. T. B. (1990). Phase-noise-free coherent optical communication system utilizing differential polarization shift keying (DPolSK). *J. Lightwave Technol.*, 8(5):691–698.
- Jacobsen, G. (1993). Performance of DPSK and CPFSK systems with significant post-detection filtering. *J. Lightwave Technol.*, 11(10):1622–163.
- Jørgensen, B. F., Mikkelsen, B., and Mahan, C. J. (1992). Analysis of optical amplifier noise in coherent communication systems with optical image rejection receivers. *J. Lightwave Technol.*, 10(5):660–670.
- Kaminow, I. P. (1990). FSK with direct detection in optical multiple-access FDM networks. *IEEE J. Sel. Areas Commun.*, 8(6):1005–1014.
- Kaminow, I. P., Iannone, P. P., and Stone, J.; Stulz, L. W. (1988). FDMA-FSK star network with a tunable optical filter demultiplexer. *J. Lightwave Technol.*, 6(9):1406–1461.
- Kavehrad, M. and Glance, B. S. (1988). Polarization-insensitive frequency-shift-keying optical heterodyne receiver using discriminator demodulation. *J. Lightwave Technol.*, 6(9):1386–1394.
- Kazovsky, L. G. (1989). Phase- and polarization-diversity coherent optical techniques. *J. Lightwave Technol.*, 7(2):279–292.
- Kazovsky, L. G., Curtis, I., Young, W. C., and Cheung, N. K. (1987). All-fiber 90° optical hybrid for coherent communications. *Appl. Opt.*, 26:437–439.
- Kazvosky, L. G., Meissner, P., and Patzak, E. (1987). ASK multipoint optical homodyne receivers. *J. Lightwave Technol.*, LT-5(6):770–791.
- Lachs, G., Henning, R. E., Choi, Y., and Zaidi, S. M. (1990). Multichannel image-rejection coherent detection system. *J. Lightwave Technol.*, 8(12):1874–1881.
- Langenhorst, R., Piper, W., Eiselt, M., Rohde, D., and Weber, H. G. (1991). Balanced phase and polarization diversity coherent optical receiver. *IEEE Photon. Technol. Lett.*, 3(1):80–82.
- Lee, J.-S. and Shim, C.-S. (1994). Bit-error-rate analysis of optically preamplified receivers using an eigenfunction expansion method in optical frequency domain. *J. Lightwave Technol.*, 12(7):1224–1229.
- Malyon, D. J. and Stallard, W. A. (1989). 565 Mbit/s FSK direct detection system operating with four cascaded photoionic amplifiers. *Electron. Lett.*, 25(8):495–497.
- Malyon, D. J.; Stallard, W. A. (1990). Multichannel FSK experiment using an optical amplifier repeater and wavelength tunable direct detection receiver. *Electron. Lett.*, 26(25):1863–1865.
- Marcum, J. I. (1960). A statistical theory of target detection by pulsed radar. *IRE Trans. Info. Theory*, IT-6(1):56–267. Earlier RAND report no. RM-753, July 1948.

- Marcuse, D. (1990). Derivation of analytical expressions for the bit-error probability in lightwave systems with optical amplifiers. *J. Lightwave Technol.*, 8(12):1816–1823.
- Marcuse, D. (1991). Calculation of bit-error probability for a lightwave system with optical amplifiers and post-detection Gaussian noise. *J. Lightwave Technol.*, 9(4):505–513.
- Martinelli, M. and Chipman, R. A. (2003). Endless polarization control algorithm using adjustable linear retarders with fixed axes. *J. Lightwave Technol.*, 21(9):2089–2096.
- Nicholson, G. and Stephens, T. D. (1989). Performance analysis of coherent optical phase-diversity receivers with DPSK modulation. *J. Lightwave Technol.*, 7(2):393–399.
- Noe, R., Heidrich, H., and Hoffmann, D. (1988a). Endless polarization control systems for coherent optics. *J. Lightwave Technol.*, 6(7):1199–1208.
- Noe, R., Rodler, H., Ebberg, A., Gaukel, G., Noll, B., Wittmann, J., and Auracher, F. (1991). Comparison of polarization handling methods in coherent optical systems. *J. Lightwave Technol.*, 9(10):1353–1366.
- Noe, R., Sessa, W. B., Welter, R., and Kazovsky, L. G. (1988b). New FSK phase-diversity receiver in a 150 Mbit/s coherent optical transmission system. *Electron. Lett.*, 24(9):567–568.
- Nussmeier, T. A., Goodwin, F. E., and Zavín, J. E. (1974). A 10.6- μm terrestrial communication link. *IEEE J. Quantum Electron.*, QE-10(2):230–235.
- Oda, K., Suzuki, S., Takahashi, H., and Toba, H. (1994). An optical FDM distribution experiment using a high finesse waveguide-type double ring resonator. *IEEE Photon. Technol. Lett.*, 6(8):1031–1034.
- Oda, K., Takato, N., and Toba, H. (1991). A wide-FSK waveguide double-ring resonator for optical FDM transmission systems. *J. Lightwave Technol.*, 9(6):728–736.
- Okoshi, T. (1985). Polarization-state control schemes for heterodyne or homodyne optical fiber communications. *J. Lightwave Technol.*, LT-3(6):1232–1237.
- Okoshi, T. (1986). Ultimate performance of heterodyne/coherent optical fiber communications. *J. Lightwave Technol.*, LT-4(10):1556–1562.
- Okoshi, T. and Cheng, T. H. (1987). Four-port homodyne receiver for optical fiber communications comprising phase and polarization diversity. *Electron. Lett.*, 23(8):377–378.
- Okoshi, T., Ishida, O., and Kikuchi, K. (1988). Simple formula for bit-error rate in optical heterodyne DPSK systems employing polarisation diversity. *Electron. Lett.*, 24(2):120–122.
- Okoshi, T. and Kikuchi, K. (1988). *Coherent Optical Fiber Communications*. KTK Scientific, Tokyo.
- Oliver, B. M. (1961). Signal-to-noise ratio in photoelectric mixing. *Proc. IEEE*, 49(12):1960–1961.
- Olsson, A. and Tang, C. L. (1979). Electrooptically tuned external-cavity CW semiconductor laser and FM optical communication. *IEEE J. Quantum Electron.*, QE-15(9):1085–1088.
- Peyton, B. J., DiNardo, A. J., Kanischak, G. M., Arams, F. R., Lange, R. A., and Sard, E. W. (1972). High-sensitivity receiver for infrared laser communications. *IEEE J. Quantum Electron.*, QE-8(2):252–263.
- Pratt, W. (1966). Binary detection in an optical polarization modulation communication channel. *IEEE Trans. Commun. Technol.*, COM-14(5):664–665.
- Proakis, J. G. (2000). *Digital Communications*. McGraw Hill, New York, fourth edition.
- Roudas, I., Antoniadis, N., Otani, T., Stern, T. E., Wagner, R. E., and Chowdhury, D. Q. (2002). Accurate modeling of optical multiplexer/demultiplexer concatenation in transparent multiwavelength optical networks. *J. Lightwave Technol.*, 20(6):921–936.
- Ryu, S. (1995). *Coherent Lightwave Communication Systems*. Artec House, Boston.
- Ryu, S., Yamamoto, S., and Mochizuki, K. (1987). Polarization-insensitive operation of coherent FSK transmission system using polarization diversity. *Electron. Lett.*, 23(25):1382–1384.

- Ryu, S., Yamamoto, S., Namihira, Y., Mochizuki, K., and Wakabayashi, H. (1991). Polarization diversity techniques for the use of coherent optical fiber submarine cable systems. *J. Lightwave Technol.*, 9(5):675–682.
- Saito, S. and Kimura, T. (1964). Demodulation of phase-modulated optical maser beam by auto-correlation technique. *Proc. IEEE*, 52(9):1048.
- Saito, S., Yamamoto, Y., and Kimura, T. (1981). Optical FSK heterodyne detection experiments using semiconductor laser transmitter and local oscillator. *IEEE J. Quantum Electron.*, QE-17(6):935–951.
- Saito, S., Yamamoto, Y., and Kimura, T. (1983). S/N and error rate evaluation for an optical FSK-heterodyne detection system using semiconductor lasers. *IEEE J. Quantum Electron.*, QE-19(2):180–193.
- Shibutani, M. and Yamazaki, S. (1989). A study on an active square-law combining method for a polarization-diversity coherent optical receiver. *IEEE Photon. Technol. Lett.*, 1(7):182–183.
- Sinsky, J. H., Adamiecki, A., Burrus, C. A., Chandrasekhar, S., Leuthold, J., and Wohlgenuth, O. (2003). A 40-Gb/s integrated balanced optical front end and RZ-DPSK performance. *IEEE Photon. Technol. Lett.*, 15(8):1135–1137.
- Siusdak, J. and van Etten, W. (1991). BER performance evaluation for CPFSK phase and polarization diversity coherent optical receivers. *J. Lightwave Technol.*, 9(11):1583–1592.
- Siuzdak, J. and van Etten, W. (1989). BER evaluation for phase and polarization diversity optical homodyne receivers using noncoherent ASK and DPSK demodulation. *J. Lightwave Technol.*, 7(4):584–599.
- Smith, D. (1987). Techniques for multigigabit coherent optical transmission. *J. Lightwave Technol.*, LT-5(10):1466–1478.
- Stein, S. (1964). Unified analysis of certain coherent and noncoherent binary communications systems. *IEEE Trans. Info. Theory*, IT-10(1):43–51.
- Toba, H., Oda, K., Nakanishi, K., Shibata, N., Nosu, K., Takato, N., and Fukuda, M. (1990). A 100-channel optical FDM transmission/distribution at 622 Mb/s over 50 km. *J. Lightwave Technol.*, 8(9):1396–1401.
- Toba, H., Oda, K., and Nosu, K. (1991). Design and performance of FSK-direct detection scheme for optical FDM systems. *J. Lightwave Technol.*, 9(10):1335–1343.
- Tonguz, O. K. and Wagner, R. E. (1991). Equivalence between preamplified direct detection and heterodyne receivers. *IEEE Photon. Technol. Lett.*, 3(9):835–837.
- Tsao, H.-W., Kuo, C.-C., Yang, S.-C., Wu, J., and Lee, Y.-H. (1992). Theoretical analysis of phase diversity optical homodyne receiver with FSK demodulation. *IEEE Trans. Commun.*, 40(4):795–809.
- Tsao, H.-W., Wu, J., Yang, S.-C., and Lee, Y.-H. (1990). Performance analysis of polarization-insensitive phase diversity optical FSK receivers. *J. Lightwave Technol.*, 8(3):385–395.
- Vodhanel, R. S. (1989). 5 Gbit/s direct optical DPSK modulation of a 1530-nm DFB laser. *IEEE Photon. Technol. Lett.*, 1(8):218–220.
- Walker, G. R., Steele, R. C., and Walker, N. G. (1990). Optical amplifier noise figure in a coherent optical transmission system. *J. Lightwave Technol.*, 8(9):1409–1413.
- Walker, N. G. and Carroll, J. E. (1984). Simultaneous phase and amplitude measurements on optical signals using a multiport junction. *Electron. Lett.*, 20(23):981–983.
- Walker, N. G. and Walker, G. R. (1990). Polarization control for coherent communications. *J. Lightwave Technol.*, 8(3):438–458.
- Westphal, F.-J. and Strebel, B. (1988). Optical heterodyne image rejection receiver. *Electron. Lett.*, 24(7):440–442.
- Willner, A. E., Desurvire, E., Presby, H. M., Edwards, C. A., and Simpson, J. R. (1990). Use of LD-pumped Erbium-doped fiber preamplifiers with optimal noise filtering in a FDMA-FSK 1 Gb/s star network. *IEEE Photon. Technol. Lett.*, 2(9):669–672.

- Willner, A. W. (1990). Simplified model of an FSK-to-ASK direct-detection system using a Fabry-Perot demodulator. *IEEE Photon. Technol. Lett.*, 2(5):363–366.
- Yamamoto, Y. (1980). Receiver performance evaluation of various digital optical modulation-demodulation systems in 0.5-10 μ m-wavelength region. *IEEE J. Quantum Electron.*, QE-16(11):1251–1259.
- Yuen, H. P. and Chan, V. W. S. (1983). Noise in homodyne and heterodyne detection. *Opt. Lett.*, 8:177–179.